AD-781 486

FOLIAGE PENETRATION (FOPEN) RADAR DETECTION OF LOW FLYING AIRCRAFT

Louis V. Surgent, Jr.

Army Land Warfare Laboratory
Aberdeen Proving Ground, Maryland

April 1974

DISTRIBUTED BY:

NTIS
National Technical Information Service
U. S. DEPARTMENT OF COMMERCE
5285 Port Royal Road, Springfield Va. 22151

UNCLASSIFIED

SECURITY CLASSIFICATION OF THIS PAGE (When Data Entered)

AD 781 486

REPORT DOCUMENTATION PAGE

READ INSTRUCTIONS BEFORE COMPLETING FORM

1. REPORT NUMBER: Technical Report 74-72

2. GOVT ACCESSION NO.

3. RECIPIENT'S CATALOG NUMBER

4. TITLE (and Subtitle): Foliage Penetration (FOPEN) Radar Detection of Low Flying Aircraft

5. TYPE OF REPORT & PERIOD COVERED: Final Report

6. PERFORMING ORG. REPORT NUMBER

7. AUTHOR(s): Louis V. Surgent, Jr.

8. CONTRACT OR GRANT NUMBER(s): None

9. PERFORMING ORGANIZATION NAME AND ADDRESS: US Army Land Warfare Laboratory, Aberdeen Proving Ground, MD 21005

10. PROGRAM ELEMENT, PROJECT, TASK AREA & WORK UNIT NUMBERS: Task 23-P-73

11. CONTROLLING OFFICE NAME AND ADDRESS: US Army Land Warfare Laboratory, Aberdeen Proving Ground, MD 21005

12. REPORT DATE: April 1974

13. NUMBER OF PAGES: 60

14. MONITORING AGENCY NAME & ADDRESS (if different from Controlling Office): US Army Aviation Systems Command, St. Louis, MO

15. SECURITY CLASS. (of this report): Unclassified

15a. DECLASSIFICATION/DOWNGRADING SCHEDULE: NA

16. DISTRIBUTION STATEMENT (of this Report): APPROVED FOR PUBLIC RELEASE: DISTRIBUTION UNLIMITED

17. DISTRIBUTION STATEMENT (of the abstract entered in Block 20, if different from Report): NA

JUL 9 1974 C

18. SUPPLEMENTARY NOTES: Work performed utilizing the LWL Multipurpose Foliage Penetration Radar developed under Task 05-P-70.

19. KEY WORDS (Continue on reverse side if necessary and identify by block number):
Radar detection of aircraft.
Nap-of-the-earch (NOE) flying.
Aircraft detection.
VHF radar.

Reproduced by NATIONAL TECHNICAL INFORMATION SERVICE U S Department of Commerce Springfield VA 22151

20. ABSTRACT (Continue on reverse side if necessary and identify by block number)

This report describes detection experiments performed with the LWL Foliage Penetration (FOPEN) Radar operating at 140 MHz in which the target was a helicopter flying nap-of-the-earth (NOE). Preliminary experiments performed in Hawaii during the user evaluation of the LWL FOPEN system demonstrated the ability of this radar to detect helicopters flying NOE using foliage and terrain for cover. As a result, the Army Aviation Systems Command sponsored a series of experiments at Aberdeen Proving Ground described in this report to establish

DD FORM 1 JAN 73 1473 EDITION OF 1 NOV 65 IS OBSOLETE

UNCLASSIFIED

SECURITY CLASSIFICATION OF THIS PAGE (When Data Entered)

20. ABSTRACT (CONT)

the detection ranges through foliage for a single UH-1 helicopter. Additional measurements of the radar cross section of the UH-1 on the ground were taken using the LWL Airborne Foliage Penetration Radar, and are also reported. The report concludes with a theoretical analysis of the propagation losses affecting the detection of aircraft flying NOE by radars operating at frequencies of from 100 to 10,000 MHz.

page iii is blank.

SUMMARY

This report describes experimental measurements and theoretical results obtained using the LWL Foliage Penetration (FOPEN) Radar to detect helicopters flying nap-of-the-earth using terrain and foliage for concealment. Tests conducted during the User Evaluation of the FOPEN radar by the 25th Infantry Division and data obtained during tests at Aberdeen Proving Ground have demonstrated that helicopters can be detected through foliage both hovering and in flight at ranges of 800 to 1,500 meters. An analysis of these results has been completed and a comparison made with known propagation losses from 100 to 10,000 MHz. This analysis, Appendix A, confirms the experimental measurements and estimates the amount of foliage necessary to prevent detection by any radar whose parameters are known. Measurements of the radar cross section (RCS) of the UH-1 helicopter taken from the airborne foliage penetration radar are presented. These show that the RCS of this aircraft with the blades turning has a maximum of 58,000 square feet depending on the illumination angle. The report concludes with a critical appraisal of the factors affecting the detection of aircraft flying nap-of-the-earth. These factors include:

a. The operating frequency of the radar

b. The amount of foliage between the radar and the aircraft

c. The height of the radar antenna

d. The height of the aircraft above the terrain

e. The radar cross section of the aircraft

f. The illumination angle (in the case of airborne or elevated radar systems)

g. The unique Doppler signatures obtained from rotary wing aircraft.

PREFACE

As a result of the preliminary detection experiments performed by the USALWL in Hawaii during the User Evaluation of the LWL FOPEN Radar, the US Army Aviation Systems Command (AAVSCOM), St. Louis, MO, sponsored additional aircraft detection tests at Aberdeen Proving Ground, MD. The assistance of Mr. A. Schlueter, AAVSCOM, who monitored and encouraged this work is acknowledged. The theoretical analysis of the detection range for aircraft through foliage, by Professor Theodor Tamir is included as the Appendix. Measurements of the radar cross section of the UH-1 aircraft taken from the air were performed by Syracuse University Research Corporation under contract #DAAD05-72-C-0299.

TABLE OF CONTENTS

	Page
REPORT DOCUMENTATION PAGE (DD FORM 1473)	iii
SUMMARY	v
PREFACE	vi
TABLE OF CONTENTS	1
LIST OF ILLUSTRATIONS	3
INTRODUCTION	5
DESCRIPTION OF THE MAN PORTABLE FOPEN RADAR (M-FOPEN)	5
DISCUSSION OF HAWAII TEST SUMMARY	11
ABERDEEN PROVING GROUND HELICOPTER DETECTION EXPERIMENTS	23
AIRBORNE MEASUREMENTS OF THE UH-1 RADAR CROSS SECTION	28
CRITICAL ASSESSMENT OF THE FACTORS AFFECTING THE DETECTION OF HELICOPTERS FLYING NOE	32
Summary	32
Discussion	32
Recommendation	34
REFERENCES	36
APPENDIX	37
Radar Detection of Low Flying Helicopters	38
DISTRIBUTION LIST	54

LIST OF ILLUSTRATIONS

Figure No.		Page
1.	Surveillance Zones with Adjustable Range Gates	7
2.	Operation Diagram, Man Portable/Multipurpose FOPEN Radar	8
3.	Major Electronic Components Man Portable/Multipurpose FOPEN Radar	9
4.	Siting of FOPEN Radar Set	10
5.	AB-577/GRC Antenna Mast used with the M-FOPEN	12
6.	M-FOPEN Radar with Data Recording Equipment	13
7.	Schematic Representation of Makua Valley Test Site	14
8.	Photograph of Test Area, Makua Valley	15
9.	Chart Recorded Data (Hawaii Test) UH-1G Aircraft	17
	REGION I Aircraft in Flight REGION II Aircraft Landing REGION III Rotor Blade Motion	
10.	Chart Recorded Data (Hawaii Test): Rotor Blade Motion, AH-1G Aircraft	18
	a. 20 seconds after engine shutdown	19
	b. 30 seconds after engine shutdown	20
	c. 40 seconds after engine shutdown	21
	d. 1 minute after engine shutdown	22
11.	Schematic Representation of Aberdeen Proving Ground Test Site	24
12.	Chart Recorded Data, (Aberdeen Proving Ground Test) UH-1 Aircraft in Flight	26
	a. 100' altitude, 1,500 meters range b. 50' altitude, 1,500 meters range c. 10' altitude, 1,150 meters range	
13.	Chart Recorded Data (Aberdeen Proving Ground Test) UH-1 Aircraft Hovering	27
14.	Airborne Target Measurement Geometry	28
15.	Radar Cross Section of the UH-1 Aircraft	30
16.	Glint Reflection Geometry	31

Preceding page blank

LIST OF ILLUSTRATIONS

APPENDIX

Figure No.		Page
1.	Two-way Additional Loss L_{bg} Over Bare Ground as a Function of Frequency	48
2.	Frequency Variation of the Attenuation and Through Vegetation	49
3.	Distance R_{100} Inside Vegetation	50
4.	Estimated Two-way Additional Loss	51
5.	Estimated Radar Loss Ptr/Prec	52
6.	Maximum Detection Range	53

LIST OF TABLES

Table No.		Page
1.	Measured RPM of the AH-1G Rotor Blade Taken From Chart Recorder Data	18
2.	Summary of the Results of the Aberdeen Proving Ground Detection Experiments	25

INTRODUCTION

Based on the helicopter detection tests performed in Hawaii using the USALWL Foliage Penetration (FOPEN) Radar, the US Army Aviation Systems Command (AAVSCOM) funded a short term program at the US Army Land Warfare Laboratory (LWL) to demonstrate the detection of helicopters flying nap-of-the-earth (NOE) using this VHF ground surveillance radar. The objectives of this program were:

a. Measure the detection ranges obtained with the FOPEN radar against helicopters flying NOE concealed by foliage.

b. Demonstrate these detections to AAVSCOM personnel

c. Provide the theoretical analysis of the factors affecting detection such as the radar frequency, radar antenna elevation and aircraft height.

d. Assess the impact on range of detection of a reduction in the aircraft radar cross section.

DESCRIPTION OF THE MAN PORTABLE FOPEN RADAR (M-FOPEN)

The M-FOPEN is a low frequency (VHF) ground-to-ground radar designed to provide the user a foliage-independent, all-weather battlefield surveillance capability. It is a coherent, pulse-doppler, moving target indicator (MTI) radar, which processes doppler returns with or without fixed returns as a reference. The radar set incorporates a 60° azimuthal beam (Figure 1) with an electronic phase monopulse to resolve individual targets to within ± 3 degrees in azimuth and a multiple target detection capability. Figure 2 is an operation diagram for the M-FOPEN, with fiberglass antenna mast and delta loop antenna. Three personnel are required to assemble and erect the telescoping AB-577 antenna tower used for the M-FOPEN aircraft detection tests. The AB-577 antenna mast is used with the M-FOPEN radar at fixed or semimobile installations where vehicle transport is available.

a. Major components (M-FOPEN)

(1) Display Box (Operator controls, azimuth readout, etc)	16 lbs
(2) Transmitter/Receiver Box (contains all RF circuitry)	16 lbs
(3) Antenna (two delta loops or log periodics required for azimuth readout)	20 lbs
(4) Antenna Mast AB-577/GRC (used for these tests in lieu of fiberglass mast used in manpack configuration)	120 lbs
(5) Control Cable (Provides for operation up to 75' from antenna base)	10 lbs

(6)	Antenna Cables	5 lbs
(7)	External Power Supply (required for 8 hrs operation)	12 lbs
	TOTAL WEIGHT	209 lbs

b. Technical Characteristics (M-FOPEN):

(1)	Operating frequency	140 MHz
(2)	Pulse width	0.15 us
(3)	Peak output power	1 kw
(4)	Average power output	8 w
(5)	Target velocity limits*	0.7 to 25 mph (40 mph with reduced sensitivity)
(6)	Maximum range (personnel & vehicles)	200 to 1,500 meters, depending on geometry, foliage, and wind conditions
(7)	Maximum range (aircraft)	2,990 meters
(8)	Minimum range	100 meters
(9)	Antenna	Array of two log periodic antennas, horizontally polarized (Figure 1) or two Delta Loops (Figure 2)
(10)	Antenna height	30-75 feet (depending on type of mast) 40 feet used for these tests
(11)	Range gates	Two, independently selectable, 20 meters wide
(12)	Azimuth coverage	60° for both inner and outer gates; 40° available for outer gate only
(13)	Target angle Azimuth readout	Angle meter readout on inner gate
(14)	Azimuth readout accuracy	Better than $\pm 5^{\circ}$, typically $\pm 3^{\circ}$

The display box shown in Figure 3 the man portable radar contains all operator controls, azimuth readout, target detection alarms, and headset capability. The operator sets each of two range gates, individually adjustable at ranges from 100 meters to the maximum range of the radar for that location, typically 200 to 1,500 meters depending on the antenna configuration, and environment. (Refer to Figure 4 for typical siting

*system modified for these tests as described in the Hawaii test summary.

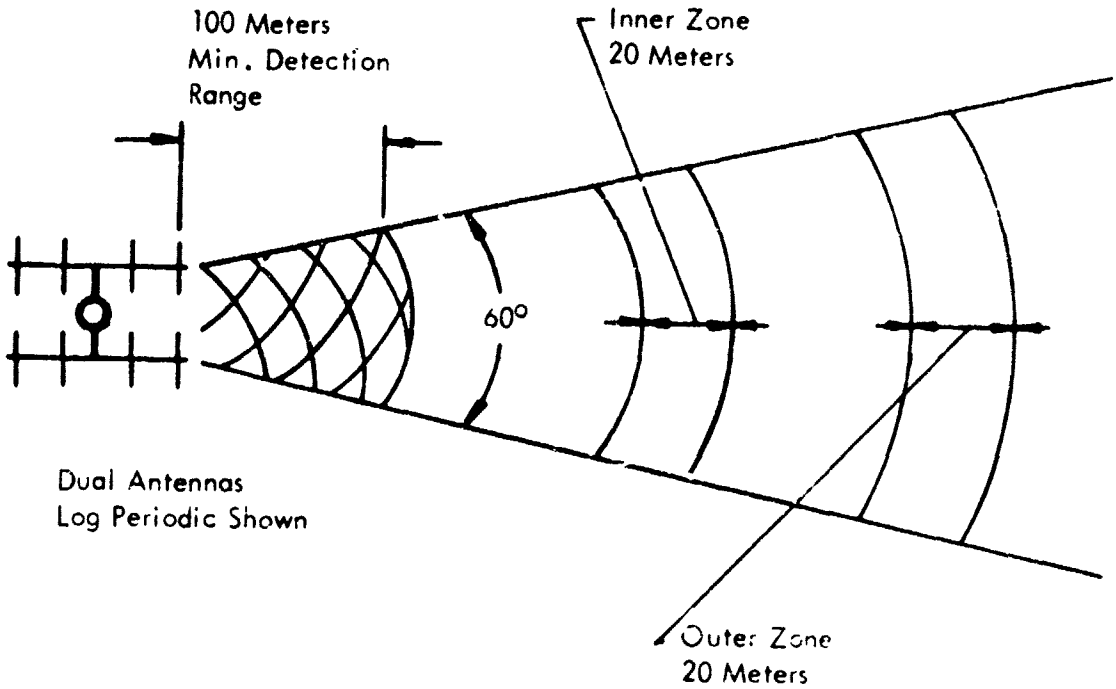

Figure 1. Surveillance Zones With Adjustable Range Zones

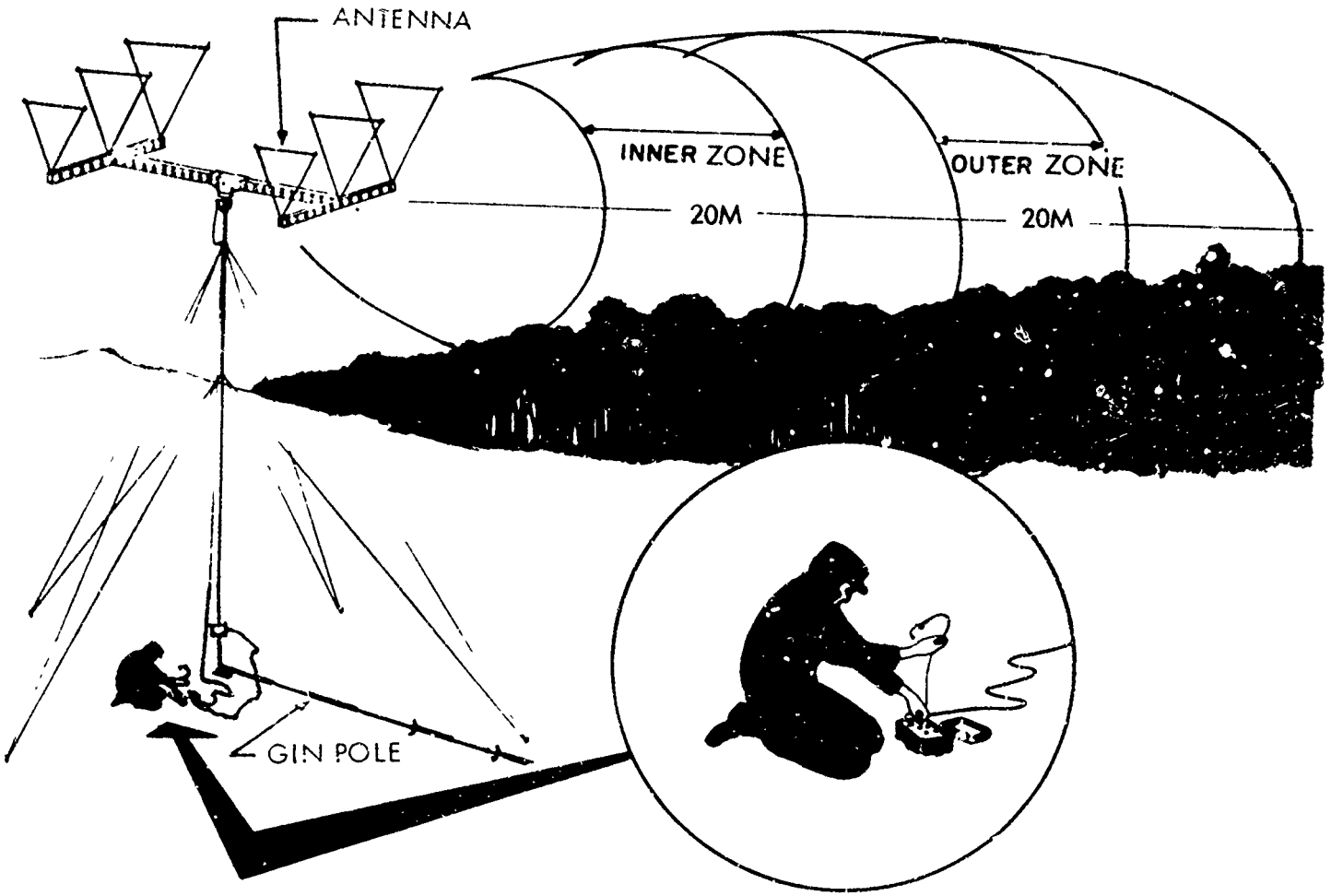

Figure 2. Operation Diagram, Man Portable Multipurpose FOPEN Radar

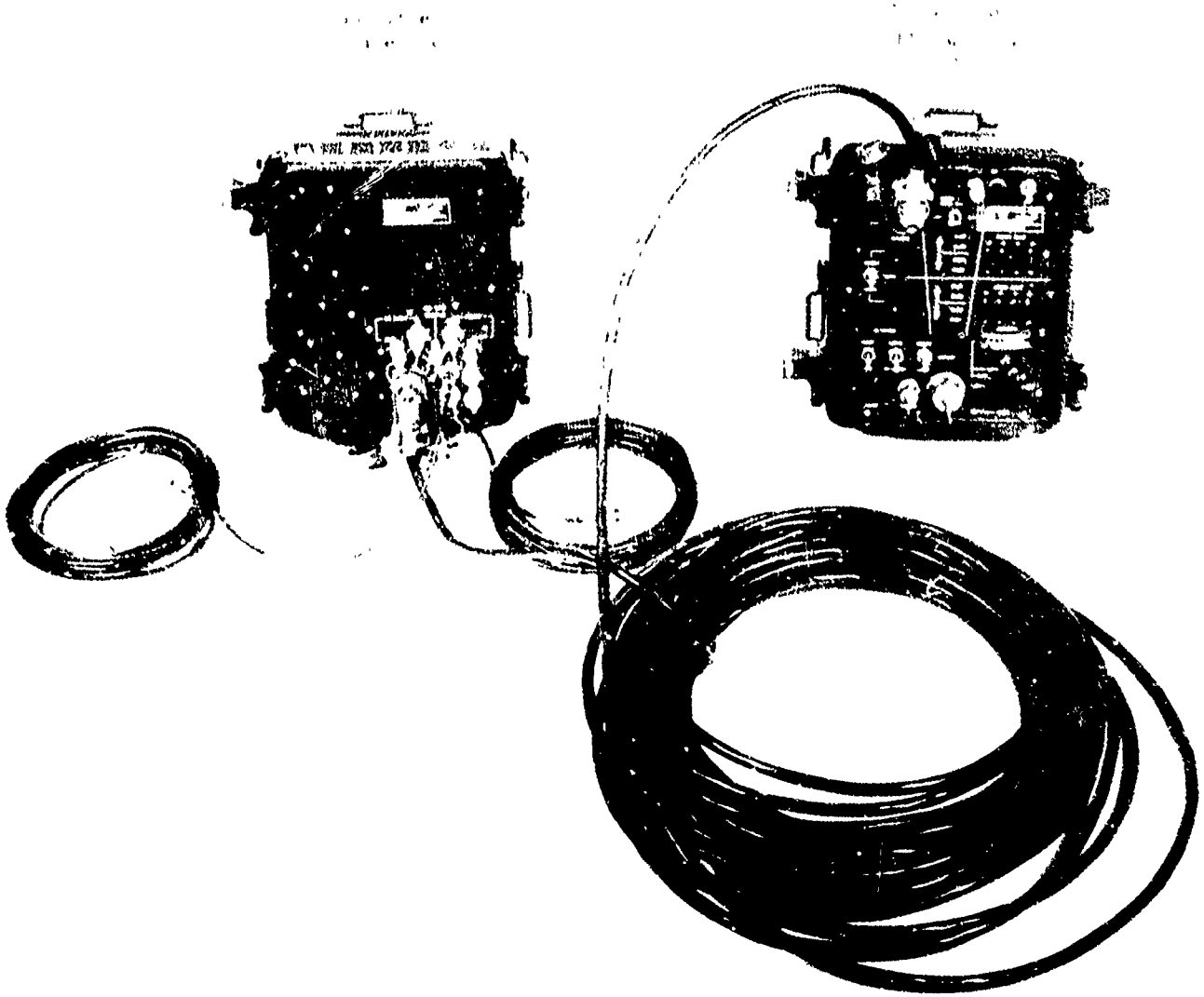

Figure 3. Major Electronic Components Man Portable/Multipurpose FOPEN Radar

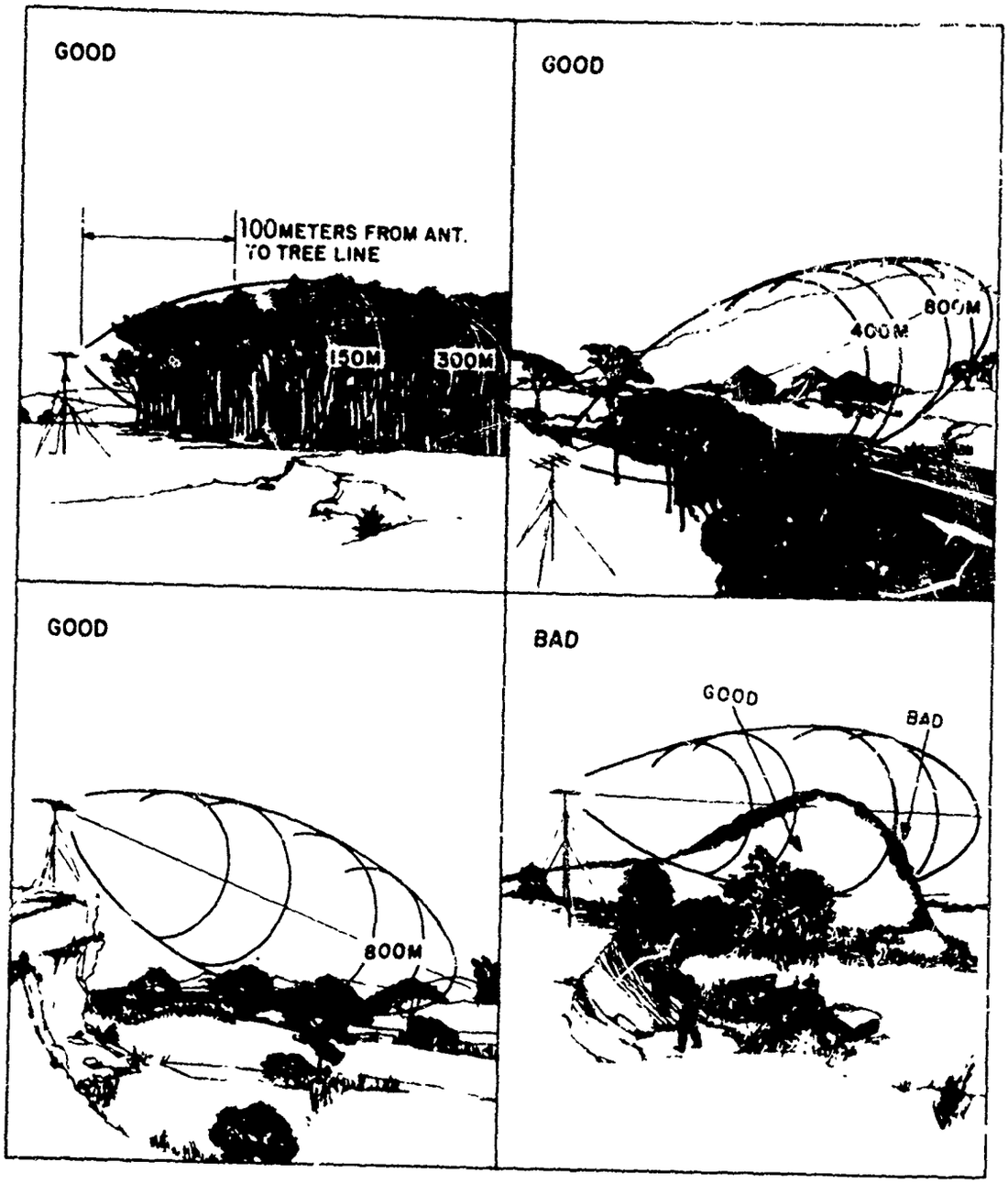

Figure 4. Siting of FOPEN Radar Set, Manpack Shown

methods). The range gates (shown in Figure 1) are 20 meters deep in a fixed 60° horizontal azimuth beamwidth which can be rotated 360° manually. The inner gate is equipped with an azimuth angle computer which provides the operator with the angle in mils left or right of the antenna direction to the target. The automatic visual and audio alarms are supplemented by the operator's headset which can be used to monitor the doppler signals from either or both range gates. Each type of target, i.e., single or multiple personnel, vehicles, etc., has a characteristic doppler signal that corresponds to its direction and velocity of motion and can be recognized by the operator. An oscilloscope is connected to the detected video and can be used for range gate positioning, target identification, determining additional information on target motion, RFI jamming analysis, and trouble-shooting the radar. For the detection experiments performed with a helicopter as the target, a chart recorder was connected to the output of the first doppler filter after the sample and hold circuits to enable both the in-phase and quadrature doppler components to be measured simultaneously.

HAWAII TEST SUMMARY

A series of detection experiments using the M-FOPEN intermediate range configuration were conducted on 2 April 1973 in Makua Valley, Hawaii, as part of the 25th Inf Division User Evaluation of these radars. During previous field testing with the radar operating through 2,000 meters of foliage, helicopters had been observed on the "A" scope oscilloscope display as a large fluctuation in the video.[1] One M-FOPEN was modified to increase the bandwidth of the sample and hold circuit to approximately 200 Hz in order to enable the higher frequency doppler information to be recorded and measured. The M-FOPEN was used with the AB/577 antenna mast shown in Figure 5 at a height of 40 feet. The radar display box was co-located with the chart recorder and "A" scope display as shown in Figure 6. Directly in front of the antenna the terrain varied upward about 3°. Line of sight was blocked by terrain masking beyond 1,100 meters. Light to medium foliage extended from directly in front of the antenna to approximately 750 meters. A roadway ran along a path parallel to the radar beam, displaced approximately 100 meters to the right. Figure 7 is a schematic representation of the site. Figure 8 is a photograph, from a small hillock located 50 meters behind the M-FOPEN antenna, showing the roadway, foliage, and the edge of the terrain mask at 1,100 meters.

On Friday, 22 March 1973, detection experiments were performed with two-target AH-1G Cobra aircraft at the Makua range. Using the "A" scope and chart recorder these aircraft were tracked at ranges out to 2,990 meters,[2] the maximum range of the M-FOPEN capability. Later, the two aircraft landed on the top of the hill at a range of 1,160 meters, and shut down their engines. The range gate was positioned over one of the aircraft and data recorded during the approach, hover, and engine shutdown. Figures 9 and 10 are samples of chart recordings made during these tests. These recordings show a unique signature for each type of aircraft activity. This clearly shows the doppler component due to the main rotor blade and

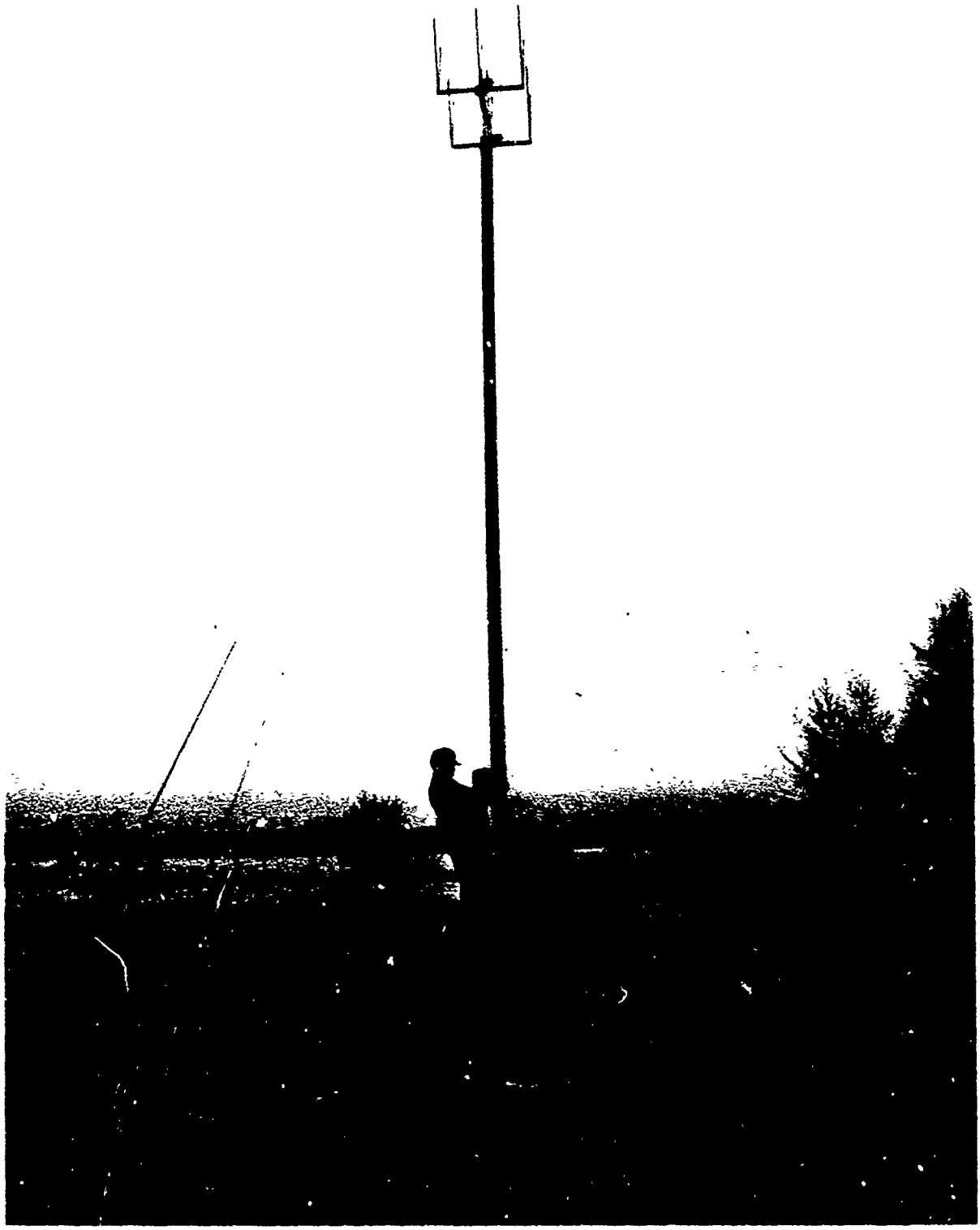

Figure 5. AB-577/GRC Antenna Mast Used with the M-FOPEN

Figure 6. M-FOPEN Radar with Data Recording Equipment

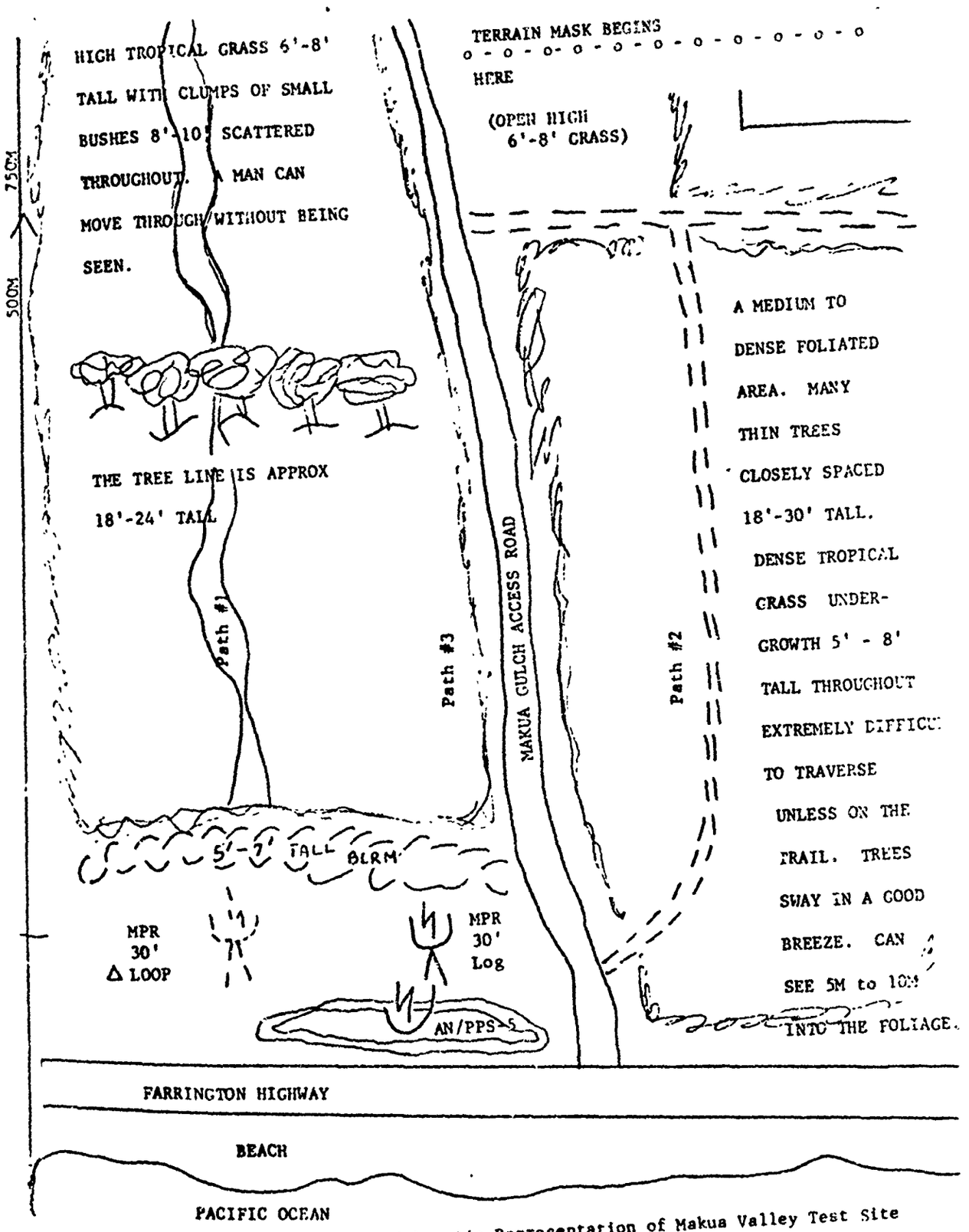

Figure 7. Schematic Representation of Makua Valley Test Site

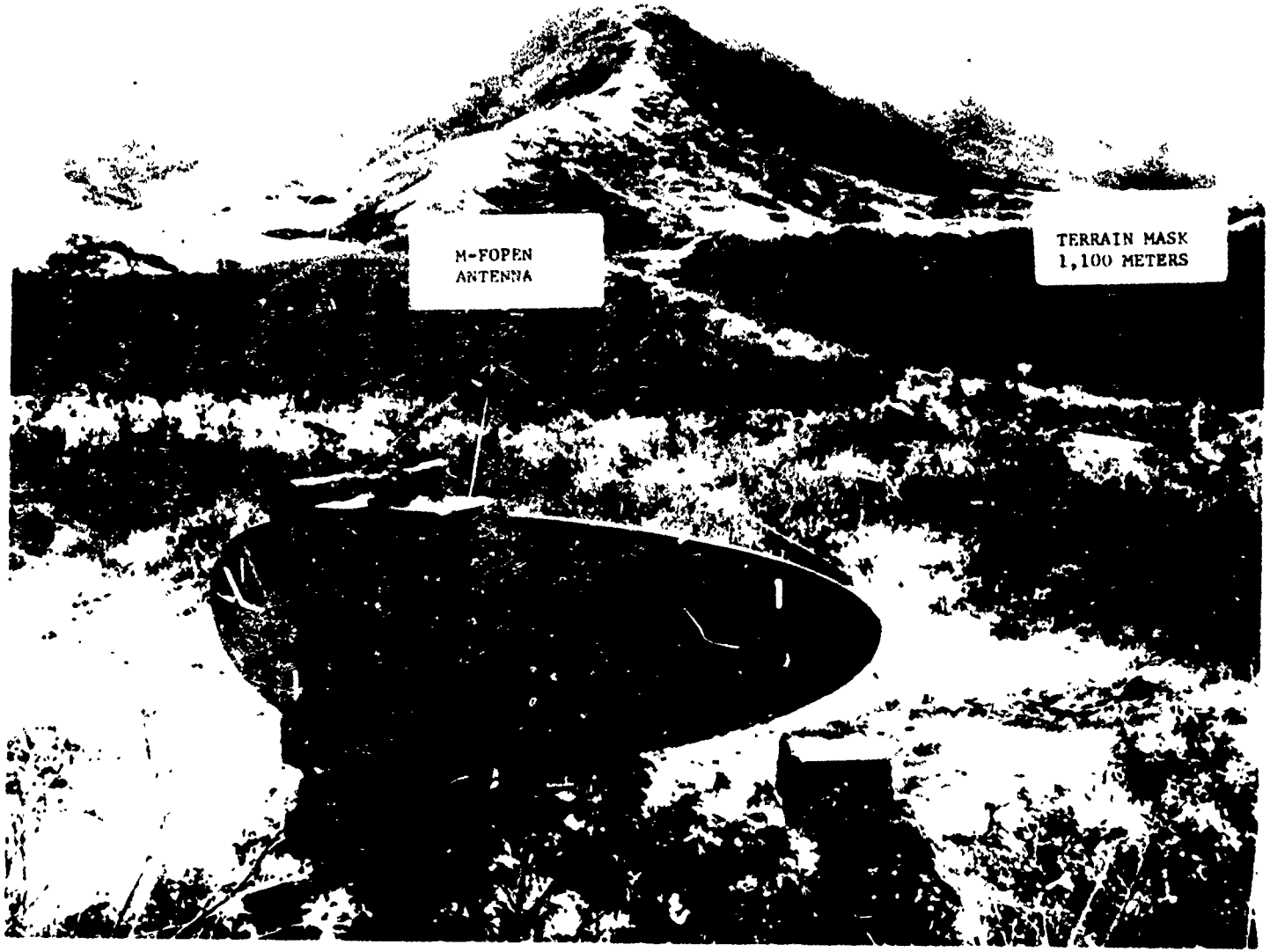

Figure 8. Photograph of Test Area, Makua Valley

also the component resulting from the motion of the aircraft. When the pilot shut down his engine the main rotor was observed on the chart recorder to slow down and stop. The energy received from the aircraft on the ground with blade turning was 2.7 times the background noise at 1,160 meters even though the aircraft was blocked from the radar by foliage and the terrain mask.

The tests clearly demonstrated the capability of the M-FOPEN and, in general, VHF radars, to detect aircraft flying behind foliage or (slight) terrain masks for concealment. As a result, one of the recommendations of the LWL FOPEN evaluation report concurred in by MASSTER,[4] was that the M-FOPEN be considered as a device to detect and identify helicopters and other aircraft.

Discussion

The data is recorded on the chart recorder from the outputs of a filter after the coherent (in-phase and quadrature) sample and hold circuits. The bandpass of this filter can be represented as shown below:

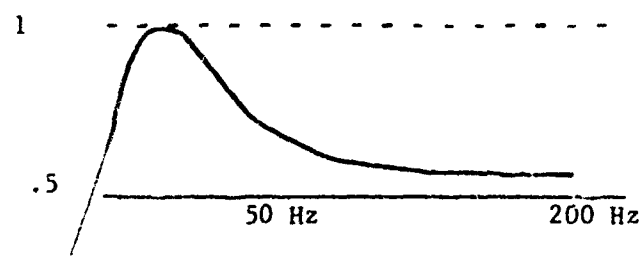

Since the amplitude response of the filter is not constant with respect to the frequency of the input signal, it is necessary to adjust the amplitude of the chart recordings before amplitude/frequency comparisons can be made.

The M-FOPEN, a phase coherent system, has a unique phase relationship between the in phase and quadrature sample and hold outputs. (A sample and hold circuit samples and stretches the video information over the reciprocal of the radar pulse repetition frequency). Representing these as vectors:

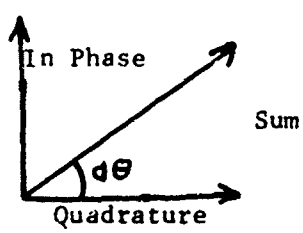

It may be shown that the direction of rotation (dθ) of the sum vector will indicate whether the target is moving towards or away from the radar. In Figure 9, a unique Doppler signature is shown for three types of aircraft motion:

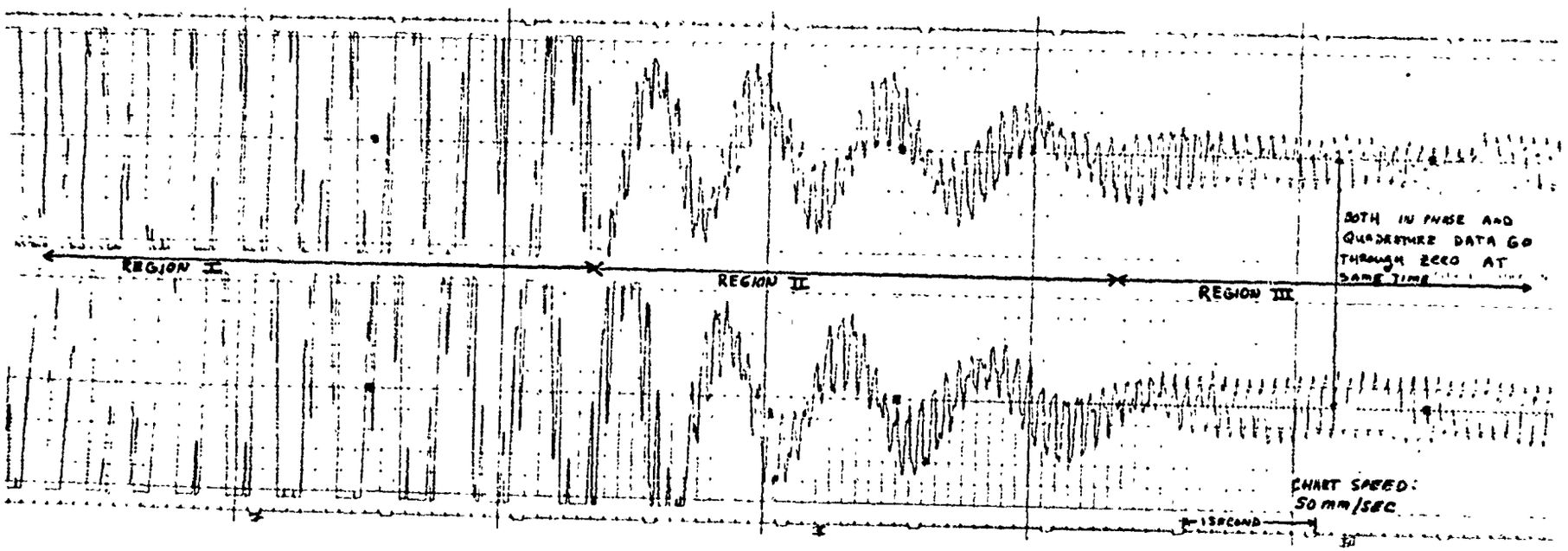

Figure 9. Chart Recorded Data
UH-1 AIRCRAFT

REGION I	Aircraft in Motion
REGION II	Aircraft Landing
REGION III	Rotor Blade Motion

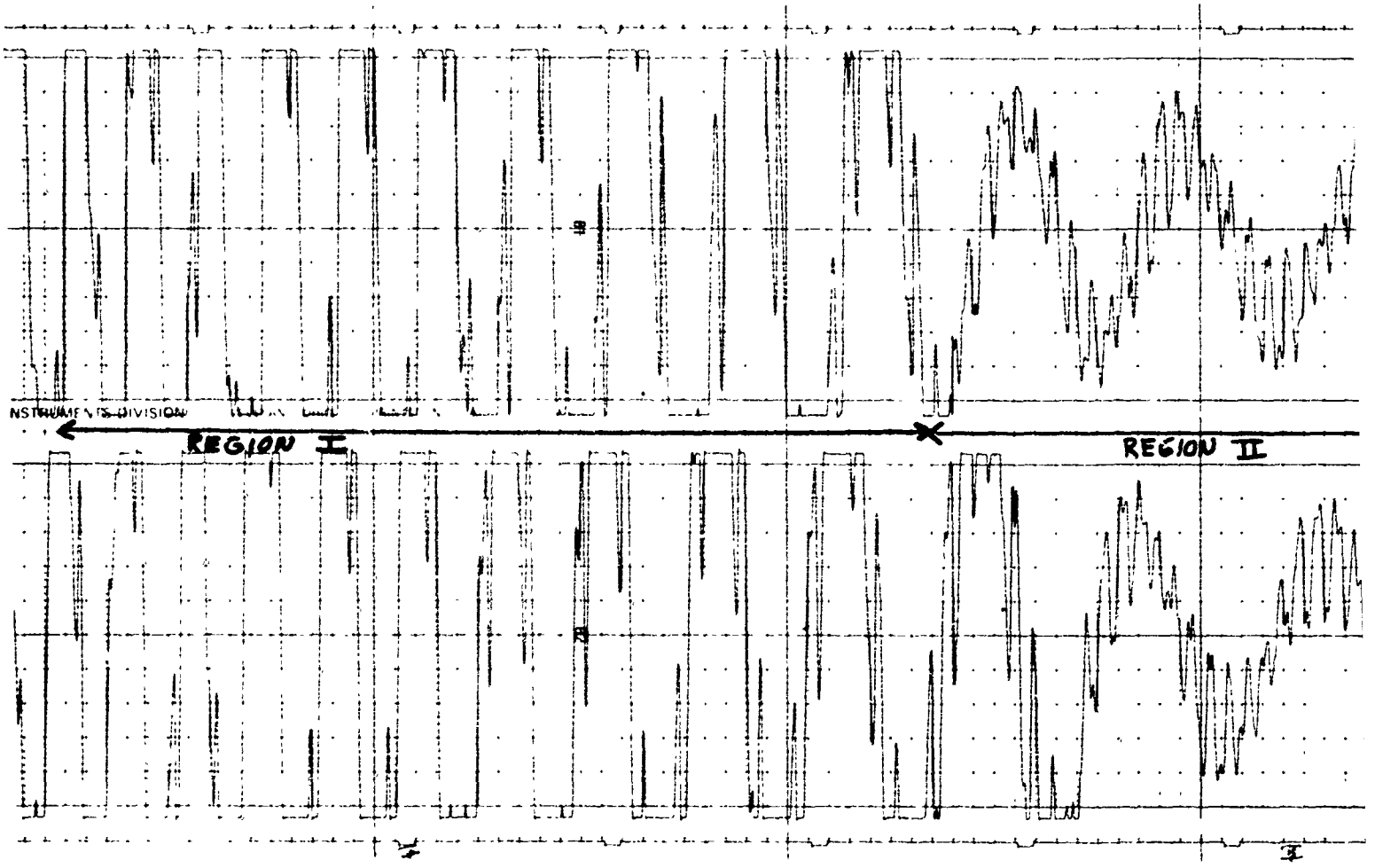
REGION I
REGION II

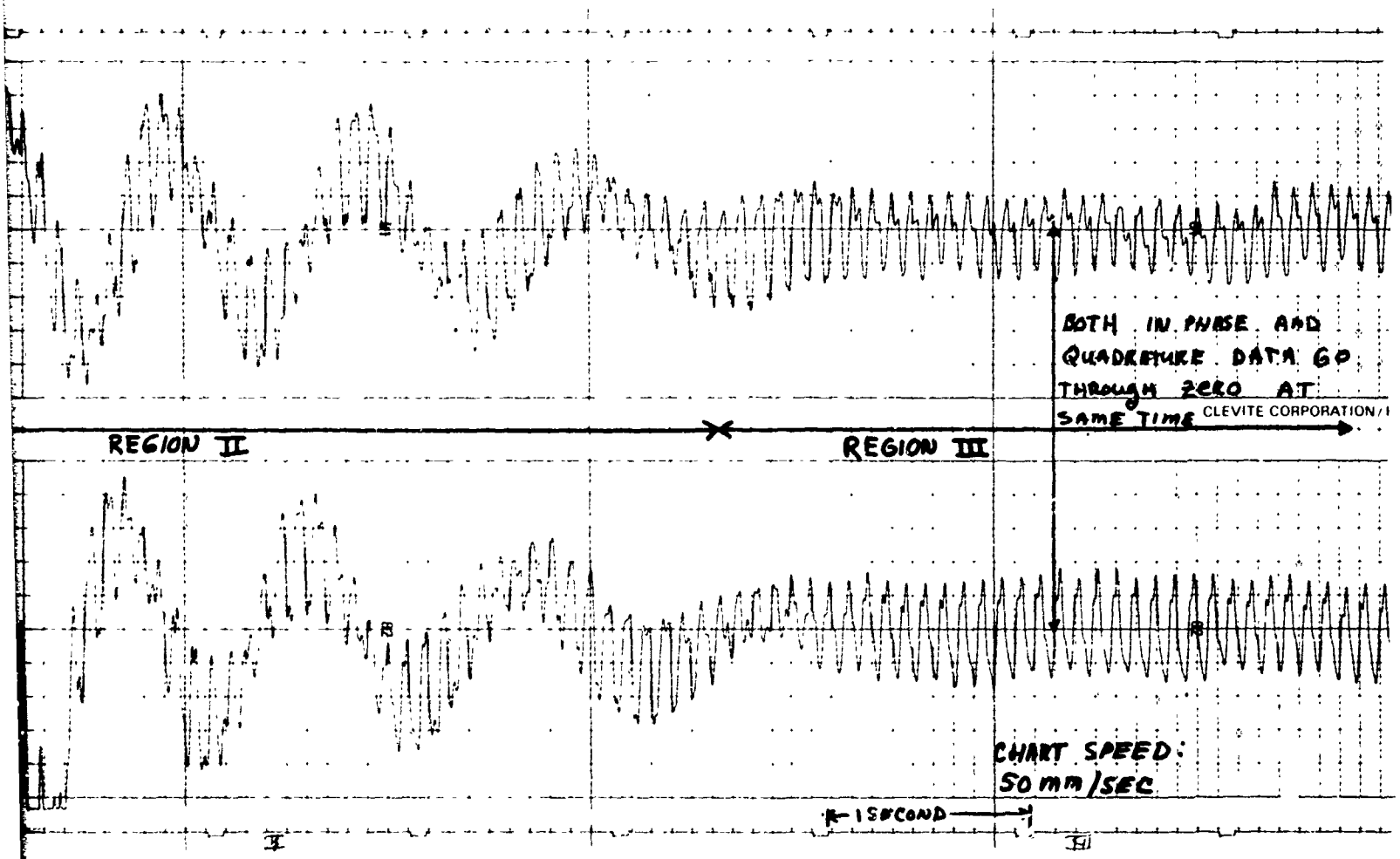

Figure 9. Chart Recorded Data
UH-1 AIRCRAFT

REGION I	Aircraft in Motion
REGION II	Aircraft Landing
REGION III	Rotor Blade Motion

REGION I: As the aircraft enters the radar range gate and goes to the hover position, the Doppler signature appears to be the rotor blade doppler modulated by the translational motion of the rotor blade and aircraft fuselage.

REGION II: As the aircraft slows prior to landing, the modulation of the rotor blade signature is reduced in frequency and intensity.

REGION III: Upon landing, the translational motion of the aircraft ceases and the doppler signature is due to the rotational motion of the rotor blade.

Notice as indicated on the data recording of Region III, that the in phase and quadrature peaks go through zero at the same instant, indicating the point of time that the blade is pointed directly in line with the radar (i.e., no net motion). This suggests that there is a specific phase relationship between the two returns which is reasonable since the blade has motion simultaneously towards and away from the observer (except when the blade is in line with the observer).

In Figure 10, a, b, c and d, four separate observations of the blade motion are shown at intervals after the aircraft has landed and shut down the engine. All recordings at the same chart recorder speed, 50 mm per second, or 1 second intervals between time marks on the margin of the chart paper. The following table gives a breakdown of the measured RPM's starting with the engine running Figure 9 and ending after engine shutdown. Figure 10d.

TABLE 1. MEASURED RPM AH-1G ROTOR BLADE TAKEN FROM CHART RECORDER DATA

Figure	Time (Approximate)	Observed CPS or No. of 1/2 blade revolutions in second	RPM (CPS x 60) No. of complete blade revolutions per minute
9	Engine running	10	300
10a	20 seconds after shutdown	8	240
10b	1 minute 30 seconds after shutdown	.83	25
10c	1 minute 40 seconds after shutdown	.67	20
10d	2 minutes after shutdown	.32	9.7

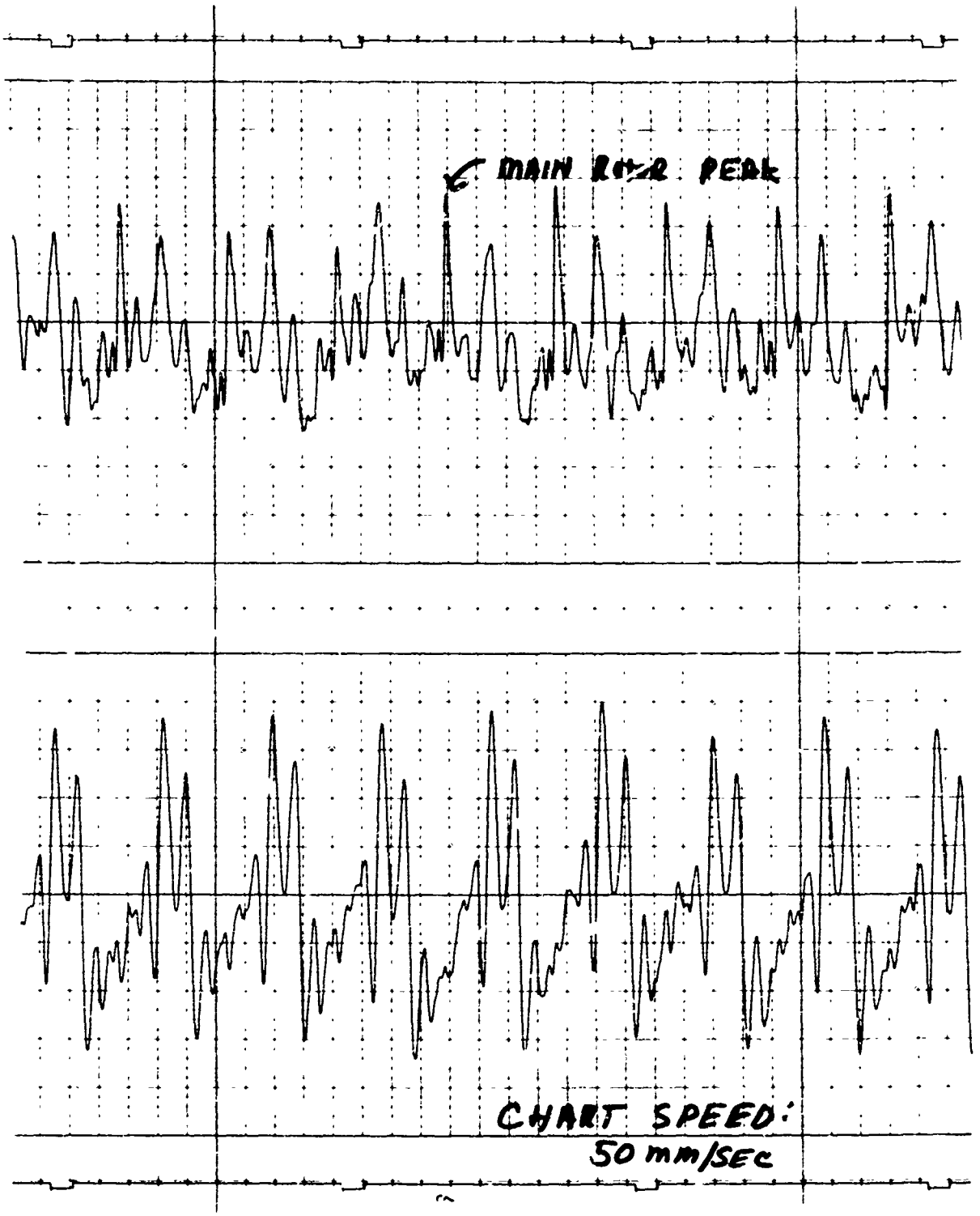

Figure 10a. Chart Recorded Data 20 Seconds After Engine Shut Down

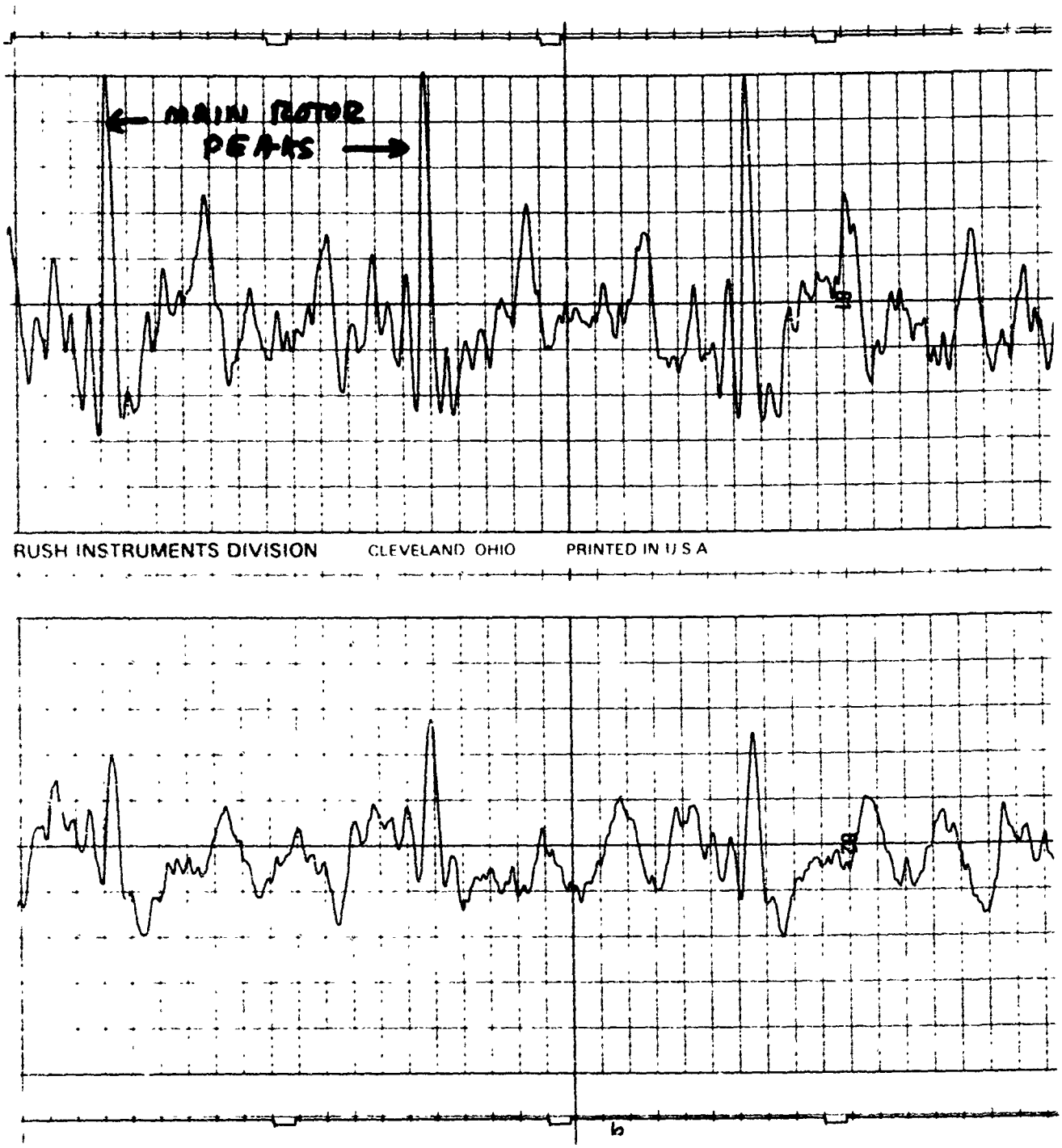

Figure 10b. 1 Minute 30 Seconds After Engine Shut Down

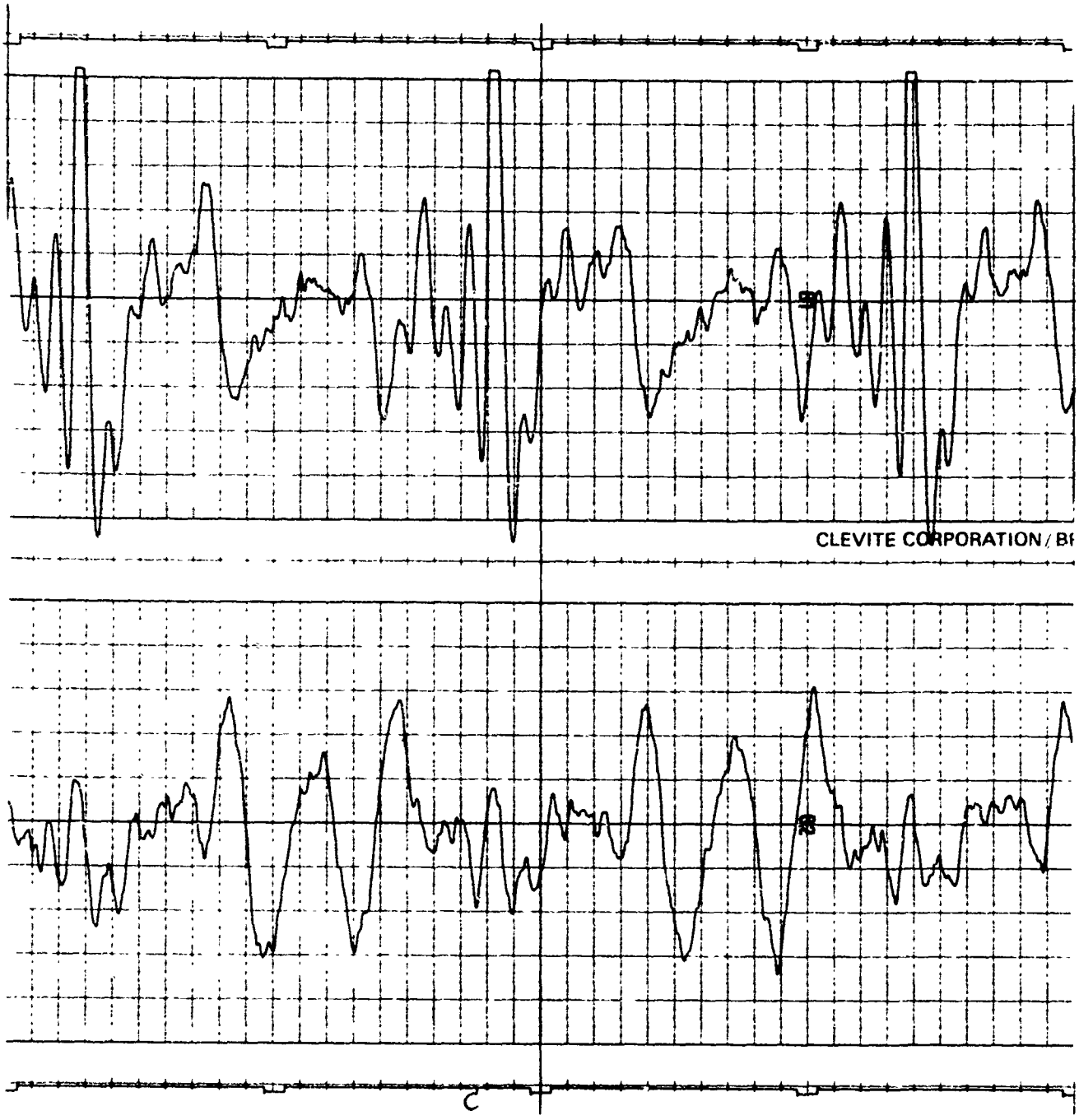

Figure 10c. 1 Minute 40 Seconds After Engine Shut Down

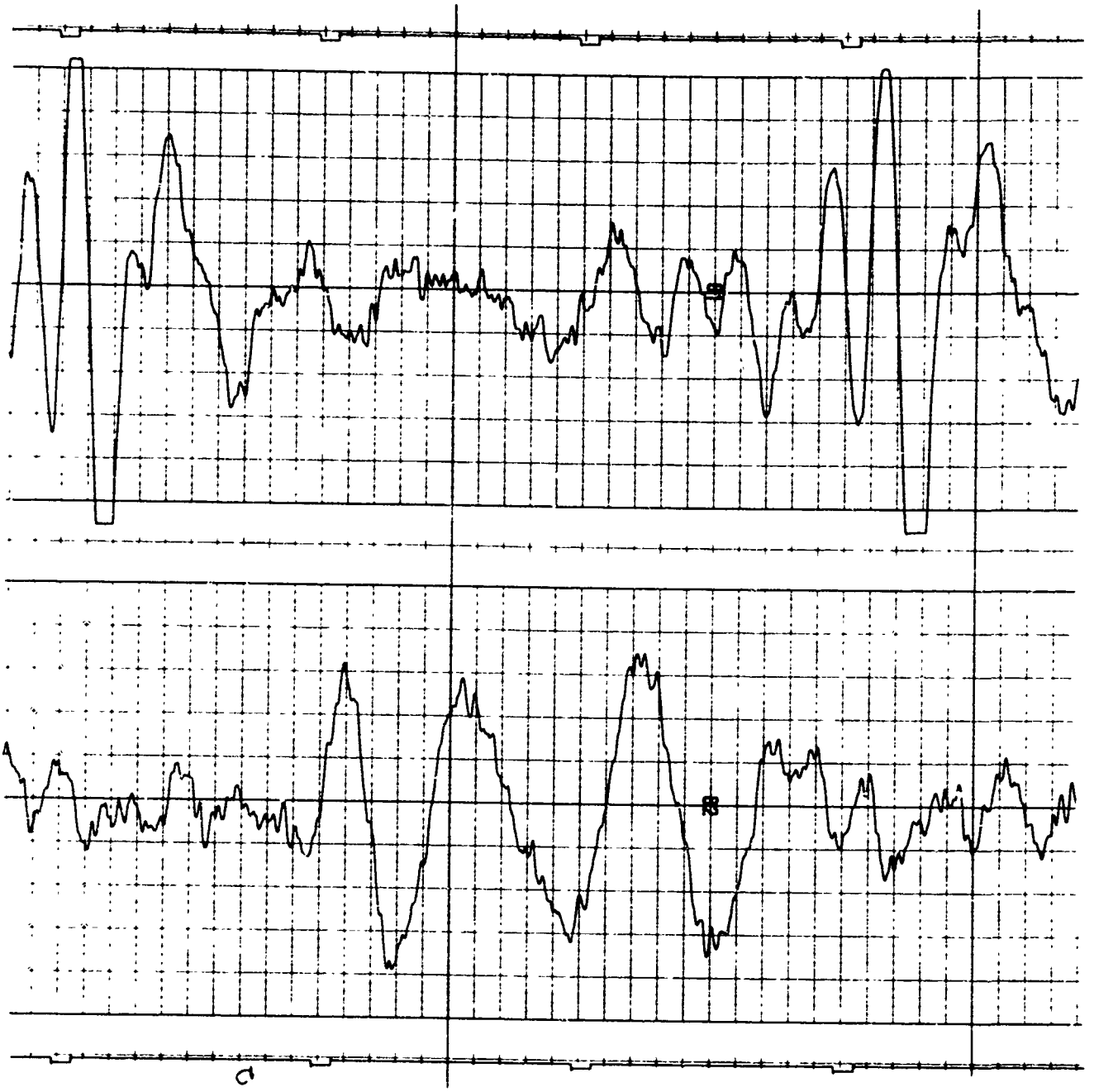

Figure 10d. 2 Minutes After Engine Shut Down

Note that each observed spike corresponds to a 180° rotation of the blade; therefore, to calculate the number of full blade rotations per minute (RPM) the number of half cycles must be divided by 2 to get full blade revolutions per second then multiply by 60 seconds per minute. These recordings show conclusively that the rotation of the rotor blade causes a unique doppler signature that can be measured accurately.

In addition, the aircraft in flight, Region I of Figure 9, appears to modulate the main rotor blade return in such a manner to enable the aircraft velocity to be estimated. Also, the lower quadrature chart recordings of c & d of Figure 10 show significant additional motion of the rotor blade not present in the upper recording of the in phase data. Evidently when the blade slows down in windy conditions, it flexes with the plane of blade rotation moving.

ABERDEEN PROVING GROUND HELICOPTER DETECTION EXPERIMENTS

Based on the helicopter detection tests performed in Hawaii, AAVSCOM, St. Louis, MO funded a short term program to demonstrate the detection of helicopters flying nap-of-the-earth (NOE) using the 140 MHz USALWL FOPEN. The objectives of this program were to determine the maximum helicopter detection ranges for radars operating in this frequency band, and to assess the effect of reducing the radar cross section of the helicopter on the maximum range of detection. AAVSCOM was concerned that certain threats operating in the frequency region 100 to 1,000 MHz could be adapted to the detection of helicopters at long ranges through foliage; possible negating the advantages of NOE flight.

Experiments were performed at Aberdeen Proving Ground to establish the maximum range of detection for a UH-1 helicopter under four conditions:

a. Hovering behind the trees

b. Flying behind a tree line

c. Flying just above the trees

d. Flying substantially (100') above the trees.

The data gathering equipment was identical to the equipment described in the previous section. The M-FOPEN with recording equipment was placed at the edge of a tree line consisting of 50' to 60' hardwoods and pines located adjacent to Bush River. The UH-1 helicopter used as a target flew two paths (refer to Figure 11), one along the water at 5' to 10' altitude, the other along a radial line at altitudes of 10', 50' and 100' over the tops of the trees. Hover tests were conducted using two cleared areas at ranges of 800 and 1,300 meters from the radar. Under the direction of the target controller, the aircraft flew inbound then outbound along the paths indicated. Aircraft velocities were from 10 to 90 kts. A target was considered to be detected when the return on the chart recorder was twice background noise.

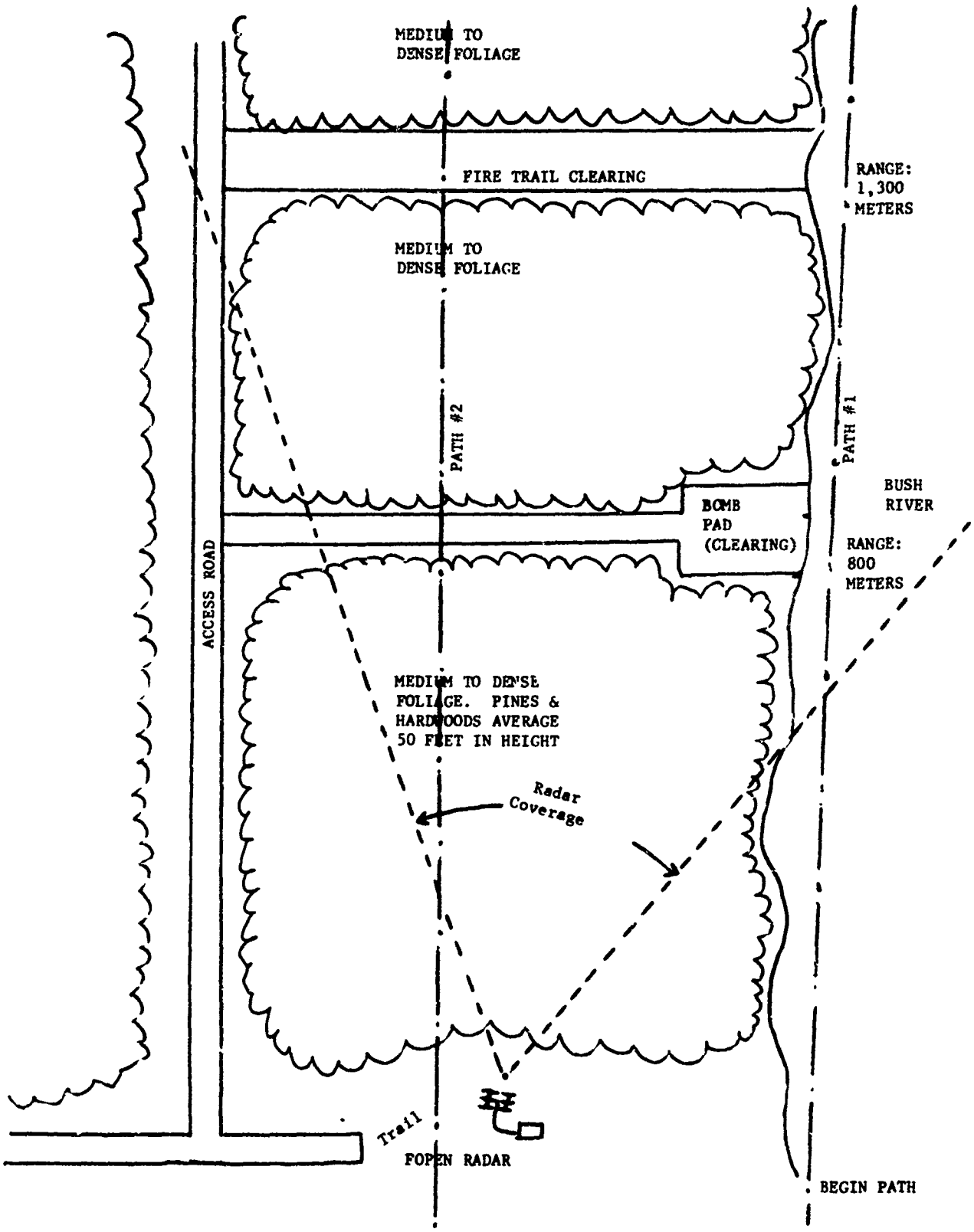

Figure 11. Schematic Representation of APG Test Site

The following Table summarizes the results of these detection experiments:

TABLE 2.
SUMMARY OF THE RESULTS OF THE
ABERDEEN PROVING GROUND DETECTION EXPERIMENTS

Target	Path	Altitude (of skids)	Max Range Detected
UH-1	Hover	2'	800M
UH-1	Hover	50'	1,300M
UH-1	#1 (along water)	5'-10'	1,200M
UH-1	#2 (over trees)	10' above trees	1,400M
UH-1	#2 (over trees)	100' above trees	2,000M

Figure 12 shows samples of the data taken that illustrate the dependence of received signal strength on the path through foliage and the height of the aircraft above foliage. The first figure shows the return from the UH-1 flying slowly at an altitude of 100' (50' above the trees) at a range of 1,500 meters. The second figure shows the return at the same range when the aircraft is flying at treetop height (50' altitude) with the skids almost touching the tree tops. The energy received with the aircraft at 100' altitude is three times that of the aircraft at 50' altitude. The last figure shows the return from the aircraft when it is flying close to the water, 10' altitude, on path 2, at a range of 1,150 meters. Although the detection occurred at 350 meters shorter range the return is 2-1/2 times less than that from the aircraft 100' above the trees and comparable with the aircraft flying at tree top level at the greater range. In the last case with the rotor and fuselage of the aircraft being completely blocked from the radar by the foliage significantly less detection range was achieved.

Detection experiments were performed with the aircraft hovering at two discrete ranges where clearings existed at 800 and 1,300 meters. The aircraft would hover at 50' altitude at each range. The radar range gate was then stepped out until the aircraft was "detected", i.e., observed on the chart recorder. Then the aircraft would gradually lower to ground level. Detections were achieved at 50' altitude for both ranges, and with the aircraft on the ground with blades turning only at 800 meters. Figure 13 is a sample of the hover at 50 feet at 800 meters. The return from the blades is very similar (in spite of a difference in chart recorded speed) to that recorded for the Cobra in Hawaii shown in Figure 9. The modulation of the characteristic rotor blade return is a result of gradual motion of the aircraft while in the hover position.

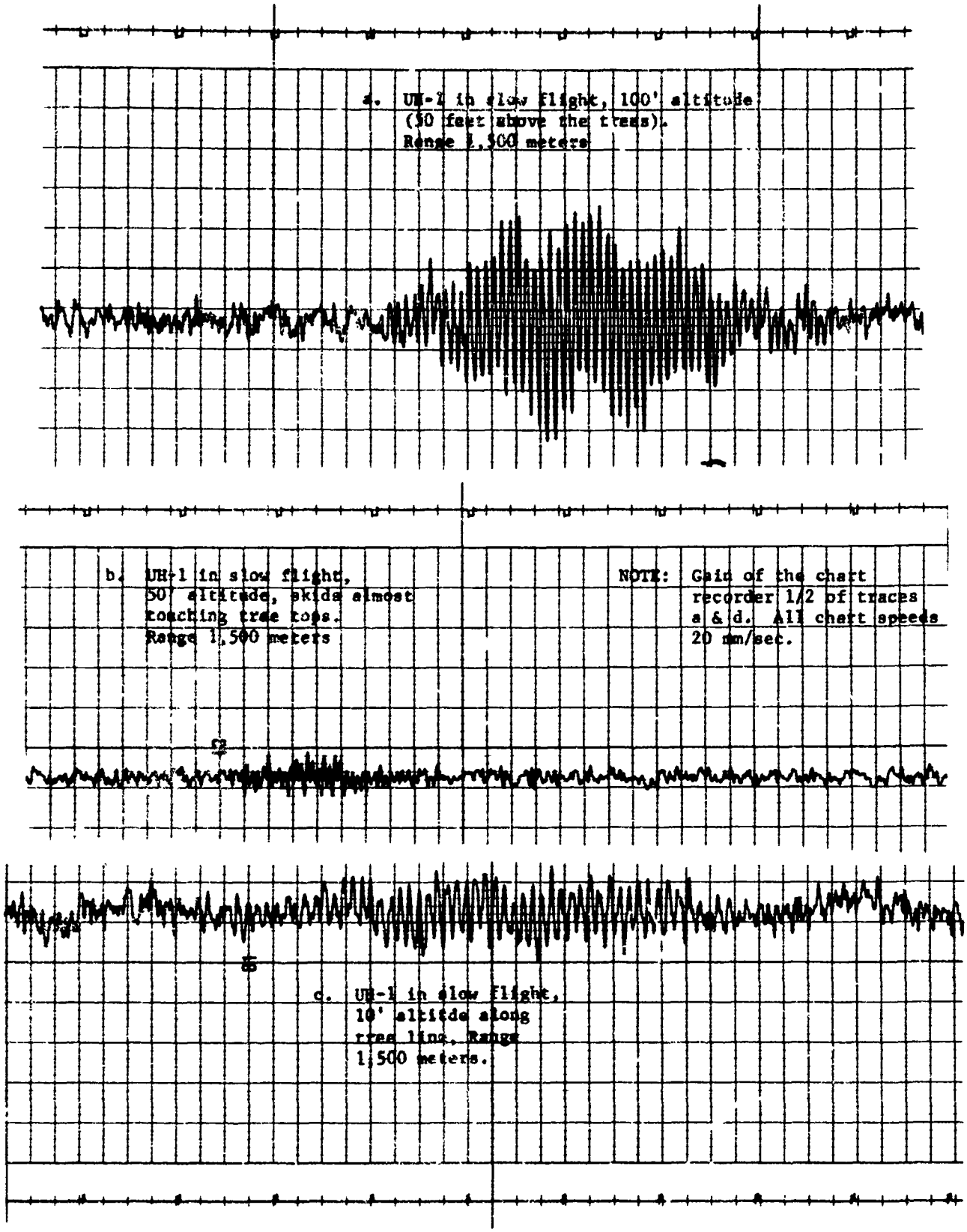

Figure 12. Chart Recorded Data, Aberdeen Proving Ground Test, UH-1 Aircraft in Flight

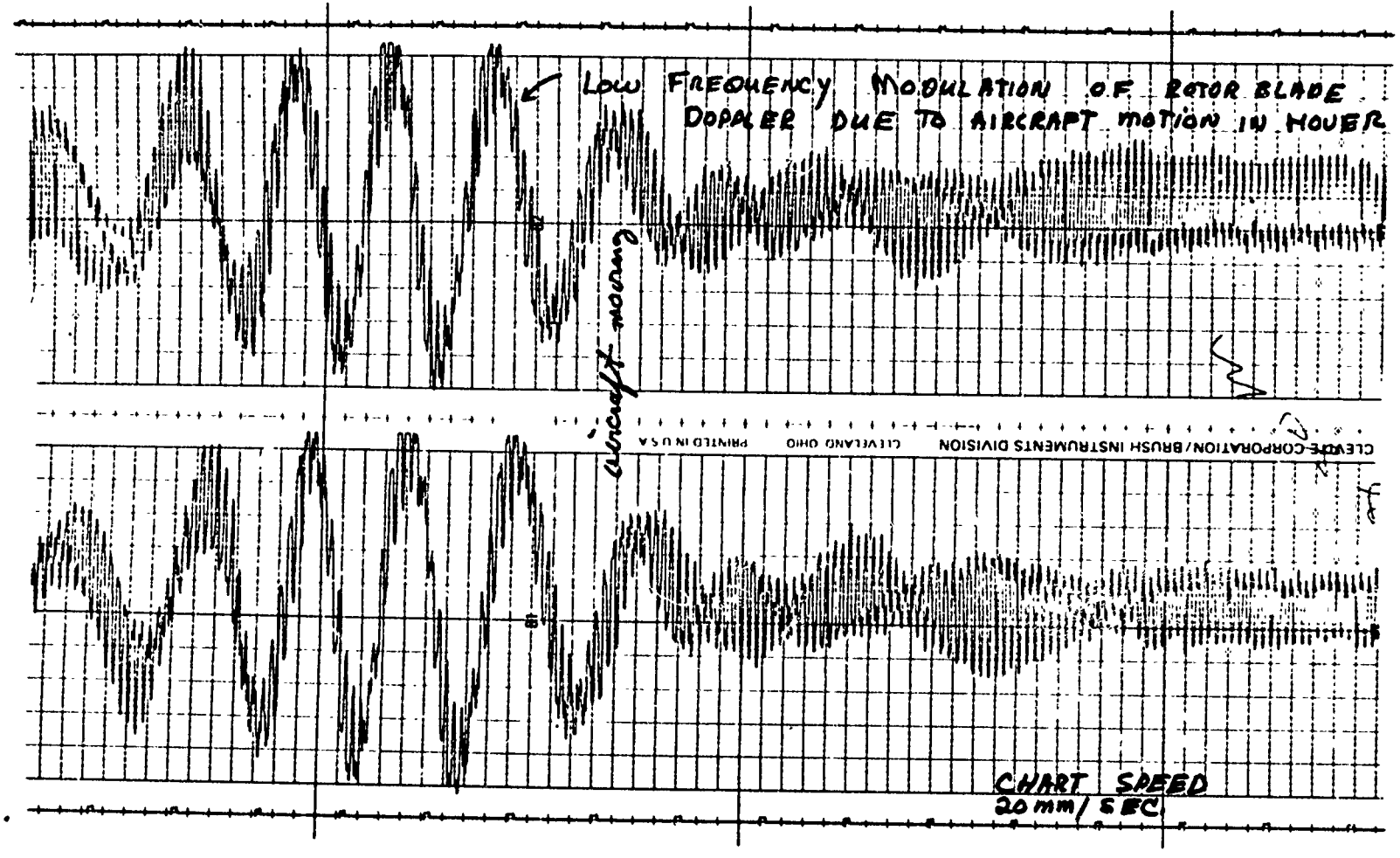

Figure 13. Chart Recorded Data, Aberdeen Proving Ground Test, UH-1 Aircraft in Flight

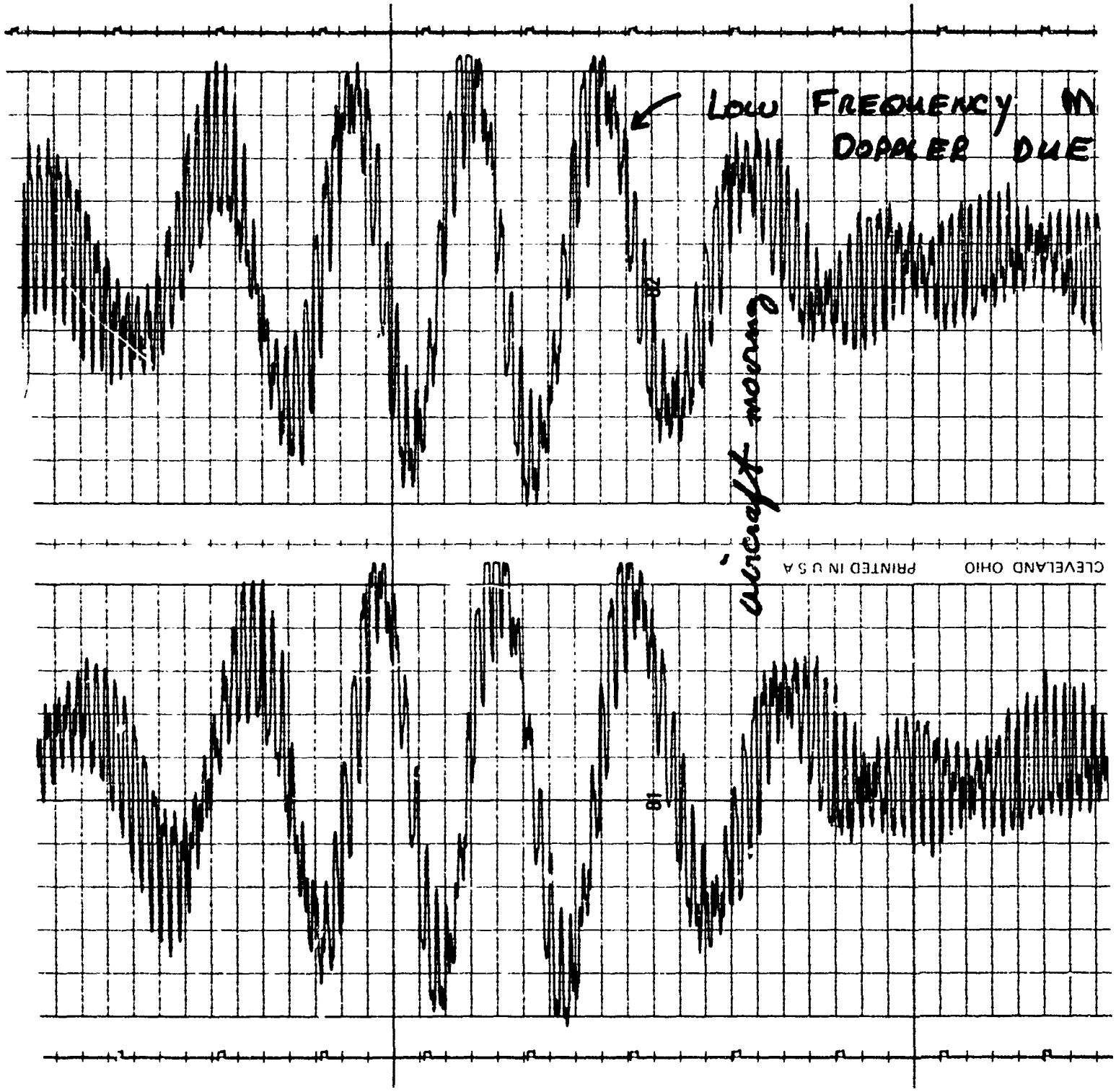
LOW FREQUENCY
DOPPLER DUE
aircraft moving
CLEVELAND OHIO
PRINTED IN U S A

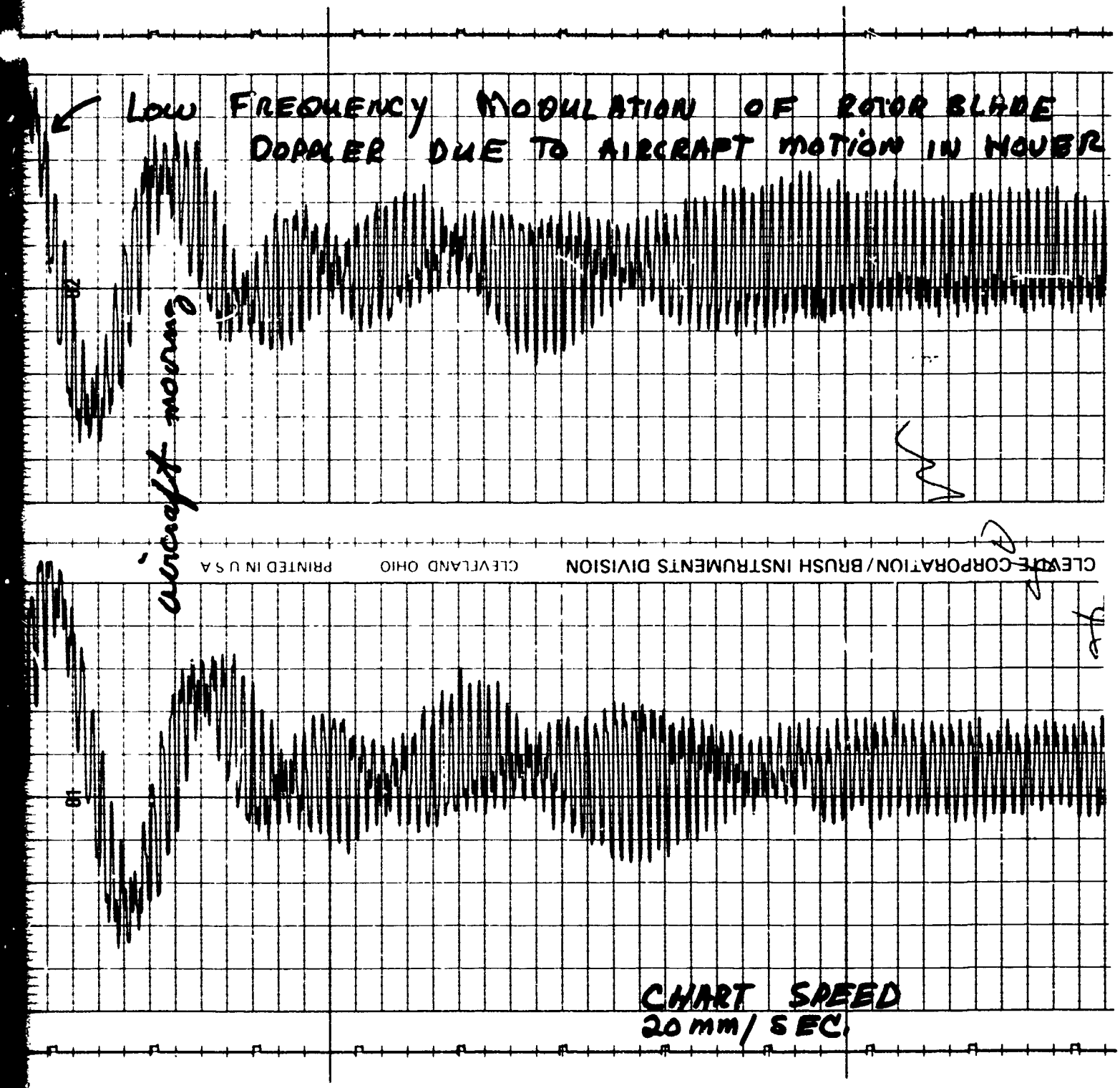

Figure 13. Chart Recorded Data, Aberdeen Proving Ground Test, UH-1 Aircraft in Flight

AIRBORNE MEASUREMENTS OF THE UH-1 RADAR CROSS SECTION

Measurements were made of the radar cross section of the UH-1 helicopter, on the ground with and without blade rotation, using the USALWL airborne foliage penetration radar system, LWL Task 07-P-72, which also operates at 140 MHz. This system was developed by Syracuse University Research Corporation under contract #DAAD05-72-C-0299. The objective of this program was to utilize the M-FOPEN Radar in an airborne role to detect both fixed and moving targets. The system was based on previous airborne detection experiments performed under contract #DAAD05-71-C-0156[5] in which a prototype M-FOPEN was mounted in a DC-3 aircraft to demonstrate the detection of targets concealed by foliage. The performance parameters of the airborne radar are similar to those of the M-FOPEN (a M-FOPEN radar is used as the RF section in the airborne system) with the exception of analog to digital converters on the outputs of the sample and hold circuits used to digitize the sampled video for recording on magnetic tape. The antenna is located on the starboard wing of the aircraft with the range gate coverage illustrated below.

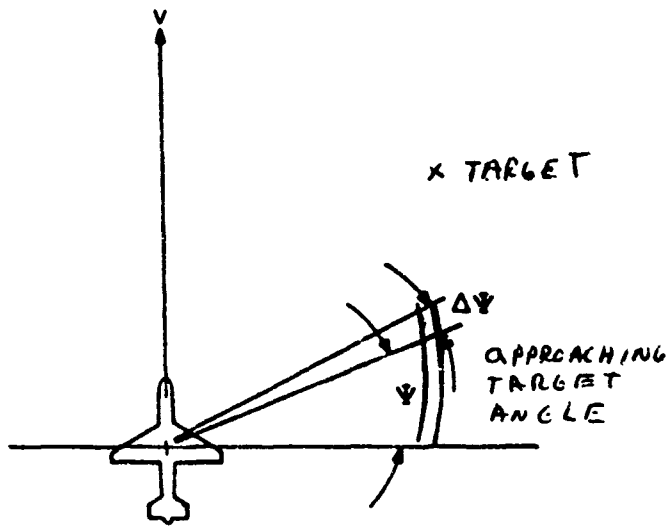

Figure 14. Airborne Target Measurement Geometry

The return from the target is determined by measuring the energy in the range and azimuth cell (approximately 100' x 100') and comparing this with a calibrated injected signal, i.e., of known amplitude.

Data was recorded on 7 and 8 March 1973 with the UH-1 helicopter located on the end of runway 22 Phillips AAF. Passes were made with the airborne FOPEN radar at two altitudes, 700' and 1,000' (slant ranges of 1,100' and 1,500'). Three separate target configurations were used: blade fixed, blade rotating at 275 RPM and blade rotating at 325 RPM. The measurement aircraft, a DC-3, flew parallel to the axis of the UH-1. All experiments indicated that the aircraft return was at least 20 dB above the background clutter. Figure 15 is a plot of the radar cross section of the UH-1 in square feet as a function of azimuth angle measured from the airborne FOPEN radar platform.[6] This figure shows that the radar cross section of this aircraft is very sensitive to the angle of illumination by the radar and whether or not the blades are rotating. With the rotor blades stationary the UH-1 has a measured peak cross section (including the glint contribution) of 46,800 square feet, at an angle of 7 degrees (receding target). Blade rotation increases the peak RCS to 58,800 square feet, shifts the peak to -17 degrees and reduces the broadside (0° angle) RCS from 2,500 square feet with blade stationary to less than 1,000 square feet with the blade rotating. At some depression angles large radar cross sections are possible from man-made targets due to a phenomena known as glint. Figure 16 shows the geometry used in the airborne tests and in the calculation of the glint RCS (with blades rotating) that follows:[4]

$$\sigma_G = \frac{16 \pi A^2}{\lambda^2} \sin^2 (90^o - \delta)$$

A = target area, perpendicular to the ground
λ = wavelength of the transmitter energy
δ = depression angle to the target

An estimate of the helicopter's surface area was determined from a photograph and a scaling factor related to the main rotor dimension.

A = side area of the helicopter, 224 square feet
δ = 14.7 degrees

$$\sigma_G = \frac{16 \pi (224)^2}{49} \sin^2 (90^o - 14.7^o) = 48,157 \text{ square feet}$$

For the experiment with the helicopter's rotors stationary, the raw data value of its maximum cross section was 46,471 square feet. The difference between the glint and the raw data values for the blade rotating indicates 10,000 square feet, due in part to the nonglint RCS of the blade. Therefore, the large value for the helicopter RCS was probably caused by the geometry of the data gathering, which resulted in a large glint contribution to the RCS.

THIS

PAGE

IS

MISSING

IN

ORIGINAL

DOCUMENT

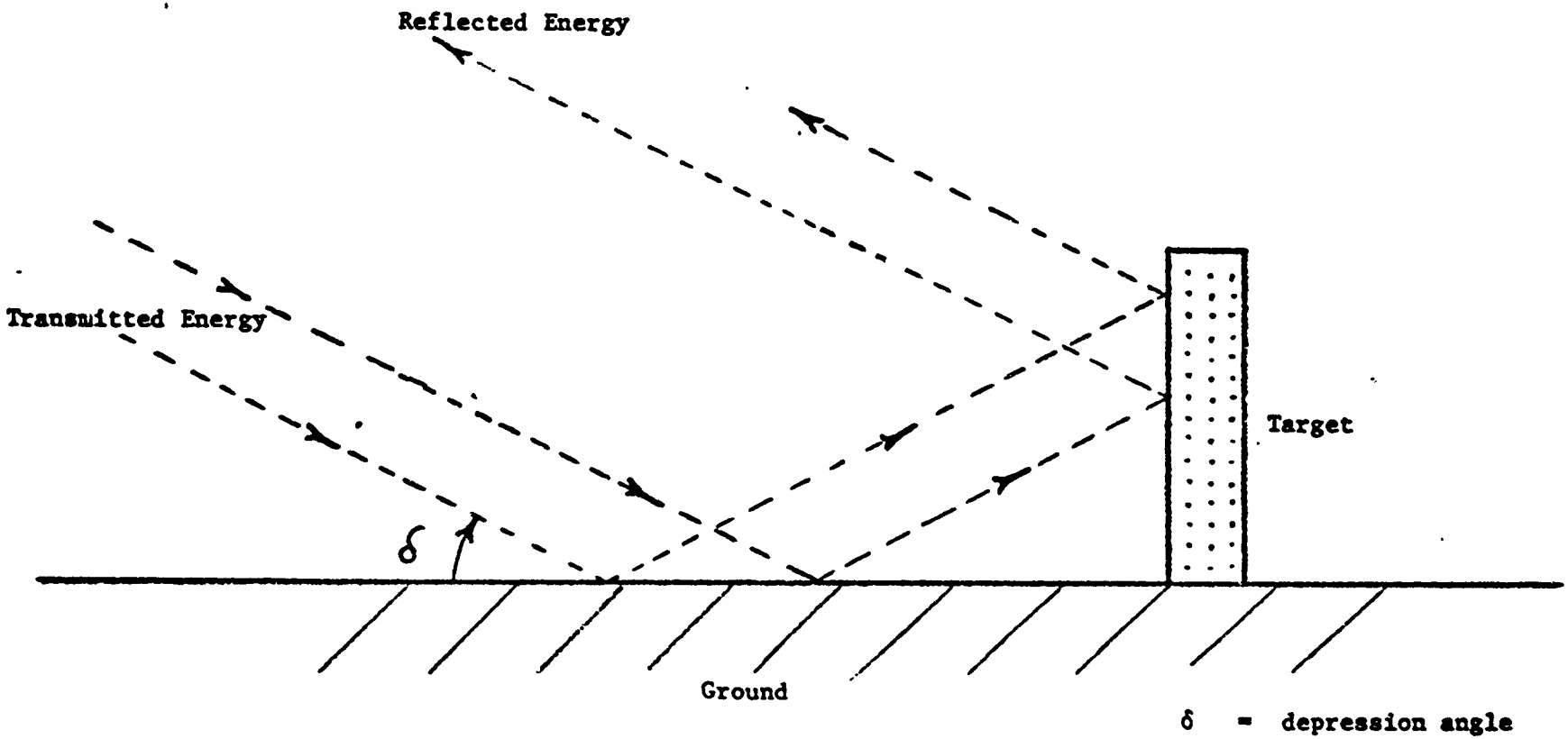

Figure 16. Glint Reflection Geometry

Although this large cross section at certain aspect angles was not anticipated, the good agreement with the glint theory supports the experimental results. This cross section is usable for detection by an airborne radar system operating in the VHF or UHF frequency region. Steps therefore should be taken to utilize tactics that would reduce the glint return such as:

. reduce the radar cross section of the rotor blade, the largest portion of the UH-1 radar return.

. aircraft should park or hover on or near rough surfaces of vegetation to reduce the glint reflection due to reflecting ground.

Assessment of the Factors Affecting the Detection of Helicopters Flying NOE

Summary

Summarizing the results of the experiments performed to date and the theoretical analysis of the Appendix, the following are the primary factors affecting the detection of aircraft:

a. The operating frequency of the radar.

b. The amount of foliage between the radar and the aircraft.

c. The height of the radar antenna.

d. The height of the aircraft above the terrain.

e. The radar cross section of the aircraft.

f. The illumination angle (in the case of airborne radar systems).

g. The unique doppler signatures obtained from rotary wing aircraft.

Discussion

The choice of the operating frequency of a radar designed to detect aircraft must be made based on a trade off between the required free space and bare ground detection ranges vs the detection range required through foliage. Looking at the two extreme cases (discussed in Appendix A) gives an idea of the numbers involved. Assuming two similar radar systems with the parameters of Appendix A, one operating at 100 MHz and one operating at 10,000 MHz.

In free space, i.e., with the helicopter high above the terrain there is a 10-fold difference in detection range:

at 100 MHz, maximum range	13 km
at 10,000 MHz, maximum range	130 km

Under these conditions the proper choice of radar frequency (or the radar posing the most serious threat to the helicopter) is the 10,000 MHz system. However, if one assumes a path through foliage, the maximum range of the 10,000 MHz system is 65 meters (theory) vs 550 meters (theory) and 800 meters (demonstrated) for the 140 MHz systems. No experimental data is available for the detection of aircraft through foliage at 10,000 MHz. The curve of Figure 6 of Appendix A can be used to determine how much foliage is necessary between an aircraft and an enemy radar to preclude detection of the aircraft. An intelligent choice of NOE flight paths can then be determine by knowing the frequency of the specific threats, having an aircraft warning receiver to know when illuminated, and some knowledge of the terrain.

If the radar antenna is located in a commanding position such as a hilltop or an airborne early warning system, and a line of sight is available between the radar and target, then the free space or modified free space (ground lobing) considerations apply, Section 1 of the Appendix, and the choice of radar operating frequency (hence the greatest threat) is the 10,000 MHz region. Unless some terrain masking can be obtained these systems can make detection under most conditions.

However, as has been encountered often in practice, weapon associated radars are generally microwave systems with low antenna heights, using foliage and terrain for concealment. Under these conditions, the detection range of these systems is <u>critically</u> dependent on the height of the aircraft above the ground or above the foliage (to prevent detection the pilot should fly with his skids touching the trees, or inches above the ground). This is clearly demonstrated by:

a. The results of the APG detection experiments that showed that a great deal of protection (to the aircraft) was afforded even at the low frequencies when the aircraft was just above the tree tops.

b. The analysis of the Appendix that confirms this height dependence in the curves of Figure 5 and Equation 9.

$$R_{max} = \left(.01 \times 10^{16} \; \frac{P_t \; G^2 \; \lambda^b \sigma}{B \; N_f \; (\omega^2 - 1)^4} \right)^{1/8}$$

As presented in the Appendix, this equation shows that the maximum detection range of an aircraft goes as the 1/8th power of the radar cross section of the aircraft σ, when the aircraft is concealed by foliage. This includes the region immediately above the tops of the trees if the radar is below the tree line. The importance of this result (confirmed by the Aberdeen experiments) cannot be over emphasized. In free space the maximum range of a radar threat goes as the cross section to the 1/4th power, thus to reduce the maximum range of detection by a factor of 2 requires only a <u>16-times</u> reduction in aircraft cross section. However, when foliage conditions prevail, and given a detection range, a factor of 2 decrease in detection range requires a <u>256-times</u> reduction in aircraft radar cross section. Thus, small changes to aircraft radar cross section are not cost effective when the aircraft is in the vicinity of vegetation. Note that under these conditions the glint radar cross section is small because of the

illumination angles of ground based system. The airborne foliage penetration data is significant if airborne early warning radars in the VHF or UHF radar regions, are to be considered as significant threats. This data indicates the primary source of radar return, i.e., the rotor blades and shows the tremendous enhancement of the return due to glint. The difference between the maximum range values calculated for the UH-1 aircraft in the Appendix and the experimental results at Aberdeen Proving Ground are a result of the radar cross section of the UH-1 aircraft being several times larger than the 100 square meters assumed in the calculation.

A significant result of the Hawaii tests is the ability of the M-FOPEN to detect the aircraft on the ground (with blade turning) behind a slight terrain mask. This is a result of diffraction by the hill and illumination of the tops of the rotor blades at angles resulting in a large radar cross section for the blades.

The nature of the doppler signature relating to its shape and rotation speed is, in the opinion of the author, unique enough to enable a radar to be built that would be very effectively discriminate between rotary wing aircraft and any other type of targets. It would also be possible to modify many existing radar systems to perform this discrimination, and, if done properly, a significant improvement in detection range to these radars may be possible due to improvement in the target to clutter ratio.

During all of the tests performed with the M-FOPEN, the chart recorder output of the signal processor reliably indicated target detections at maximum detection ranges where the "A" scope only detected those targets clearly above the foliage. This is further confirmation of the necessity for advanced signal processing for radars designed to detect aircraft.

Recommendations

The results indicate a high degree of vulnerability of rotary wing aircraft to radar threats under various conditions of terrain and foliage. It is obvious that the most significant reduction in rotary wing detectability would be obtained from a redesign of the rotor blade. Such a design would probably employ shaping to reduce leading/trailing edge cross section, and radar transparent material for the body of the blade such as those manufactured by Windecker Industries of Midland, TX and evaluated by the Land Warfare Laboratory.

The most logical next step in the work reported herein would be to develop a simple table with radar threats plotted vs the amount of terrain/foliage required to negate their effects. Such a table could be derived from information already available and confirmed experimentally.

It is recommended that future warning receivers cover the low frequency radar threats and provide some indication to the pilot of the received signal level. Depending on the proximity of the aircraft to the foliage, the radar range equation will depend on some power from $p^{1/4}$ to $p^{1/8}$ (equation 8 of the Appendix). Considering the difference in the returned

path loss inherent in such a relationship, some computation of the actual probability of detection by the radar should be available to the pilot in addition to an indication that he has been illuminated by a radar system.

REFERENCES

1. Surgent, L. V., Jr., LWL Hawaii Evaluation Report: User Evaluation of the Multipurpose Foliage Penetration Radar M-FOPEN, MASSTER Test No. 77, Applied Physics Branch, US Army Land Warfare Laboratory, Aberdeen Proving Ground, MD 21005, 25 Sep 73. (To be published as USALWL Technical Report, LWL #74-73).

2. Surgent, Louis V., Jr., op. cit.

3. Surgent, Louis V., Jr., op. cit.

4. CPT William C. Bartel, LWL Hawaii Evaluation Report: User Evaluation of the Multipurpose Foliage Penetration AFMAS-CSS-L, MASSTER, Ft. Hood, TX 76544, 13 Dec 1973.

5. W. L. Emeny; G. H. Naditch, Syracuse University Research Corporation, Moving Platform Investigation for FOPEN Radar, Technical Report LWL-CR-07P72, Final Report, April 1972, AD 901593L.

6. Moving Platform FOPEN Radar Prototype Development, Syracuse University Research Corporation, SURC TD-73-179, Letter Report, Contract DAAD05-72-C-0299, May 1973.

APPENDIX

RADAR DETECTION OF LOW FLYING HELICOPTERS

The present Memorandum discusses wave propagation losses in the case of radar detection of helicopters flying at low altitudes. In particular, we shall consider helicopters that fly nap-of-the-earth, or are otherwise trying to conceal their presence by flying close to vegetation, skirting around clumps of trees or making use of forest clearings. In this context, an attempt is made here to assess the restrictions that the presence of vegetation imposes on radar systems operating in the range of 100 MHz. to 10 GHz. Specifically, the effect of the operating frequency on the detection range of low flying helicopters is critically examined.

1. Bare-Ground Terrain.

When vegetation is absent, low flying helicopters reduce their detection susceptibility by hiding behind hills or other ground irregularities. In such a case, however, it can be assumed that the radar antenna is installed on the highest convenient geographical promontory. We shall therefore not consider here the possibility of the helicopter becoming invisible because such a situation can be assumed to be, at most, of short duration only.

On a bare-ground and flat terrain, a low flying helicopter may be less easily detected than one at a higher altitude because of the ground-lobing effect on the radar antenna. This effect introduces a two-way loss L_{bg} above free space losses which, as given by Eq. (47) of reference 1, is given by

$$L_{bg} = 2\ L_{gr} = -\ 40 \log \left(2 \sin 2\pi \frac{z z_o}{\lambda R}\right) , \qquad (1)$$

where z and z_o are the heights above ground of the helicopter and radar antenna, respectively, λ is the wavelength and R is the range (distance between the antenna and the target). The loss L_{bg} is shown in Fig. 1 for a typical case with $z = 3$ meters, $z_o = 10$ meters and for several values of R. For other combinations of z, z_o and R, the parameter $a = zz_o/R$ (all quantities in meters) can be used, as given by the values shown in brackets in Fig. 1.

It is obvious from Fig. 1 that, because of the ground-lobing effect, it is preferable to operate the radar at the higher frequency end, i.e., around 10 GHz. or higher. However, it is worthwhile to note that the loss L_{bg} is not too large if the range R is small. Thus, for $R < 1$ km., L_{bg} is less than 40 dB. for $f \geq 100$ MHz. This indicates that ground-lobing losses may be tolerable at the lower frequencies around 100 MHz. As we shall see further below, the presence of vegetation causes severe losses at the higher frequencies, such losses being by far larger than those produced by ground lobing at the lower frequencies.

2. Fully Vegetated Terrain.

When the terrain contains a large forest, low flying helicopters can often interpose between themselves and the radar antenna a path that lies entirely through vegetation. In such a case, the clutter and the absorption produced by vegetation cause a drastic reduction in the detection range.

The problem of clutter can be substantially alleviated by using radar systems that perceive moving targets by means of the Doppler-shifted frequency of the return signal. To further improve the detection capabilities, it is also necessary to use a balanced processor in the radar receiver, which helps suppress Doppler-shifted signals due to trees swaying in the wind and/or other objects that have an oscillatory movement, i.e., with a zero average displacement. We shall therefore assume in the following that such a system is being used, so that the problem of clutter will not be discussed further.

Because a signal traveling through vegetation is scattered in essentially all directions, only a small portion of its energy can reach the target. This scattering mechanism is additional to the attenuation of the wave, which is caused by the signal having to penetrate through the vegetation, which exhibits ohmic losses. Both these ohmic losses and the scattering losses combine to yield a total loss that produces a strong attenuation of the signal, which is measured by the attenuation constant α (in dB.). To assess this loss, consider Fig. 2 which describes concisely the (unfortunately, very few) available propagation data through foliage for frequencies above 100 MHz. In Fig. 2, the total attenuation α is plotted as function of frequency in the frequency range of interest here. It is seen that the spread of measured values of α is quite large, e.g., it varies between 0.25 to 0.48 dB./ meters at 1 GHz.

To obtain some estimate of the behavior of the vegetation losses, we shall therefore adopt a simplified model based on the measured data. This model is shown by the dot-dashed line in Fig. 1, which obeys the simple relationship

$$\alpha \text{ (dB./meters)} = (f_{GHz}/\ 10)^{1/2} \qquad (2)$$

By using this formula, it is easy to plot a graph of the distance R_{100} for which a two-way terrain loss L_{t2} of 100 dB. is produced by the vegetation, in addition to the free-space loss. This graph is shown in Fig. 3, wherein we see clearly that the detection range decreases rapidly with the frequency f.

To consider only a few cases, we note in Fig. 3 that R_{100} is only 50 meters at 10 GHz. This should be compared to 500 meters at 100 MHz. Furthermore, we should also recall that, for frequencies below 1 GHz., the propagation path is usually via a lateral wave[2-4] which is considerably less attenuated than the "through-the-vegetation" path assumed here. This is also indicated in Fig. 3 by the dashed portion of the line, which implies that the values shown for R_{100} are smaller than those achieved in actual practice. Figure 3

thus clearly indicates that, at the higher frequencies, severe restrictions are imposed for detecting targets along paths that lie entirely through vegetation.

A further illustration of the foregoing considerations is shown in Fig. 4. Here we have examined three different ranges, namely R = 50, 100 and 200 meters, and the two-way loss L_{t2} (above free space) due to the presence of vegetation has been calculated. From Fig. 4, it is seen that the loss L_{t2} at 1 GHz. is tolerable (= 30 dB.) for R = 50 meters, it becomes quite high (= 60 dB.) for R = 100 meters, and takes on a prohibitively high (= 125 dB.) value for R = 200 meters. This again confirms that radar detection under these conditions is questionable (and most likely impossible) for frequencies above 1 GHz.

3. Partly Vegetated Terrain.

To obtain a better comparative picture on the extent of vegetation losses, and in order to assess the effect of a partially (rather than fully) vegetated propagation path, we present in Fig. 5 the total radar path loss L for several different cases. Here, the total loss is given by

$$L = \frac{P_{tr}}{P_{rec}} , \qquad (3)$$

where P_{tr} and P_{rec} refer to transmitted and received powers, respectively. Curves of L versus f have been calculated for two ranges R = 100 and 200 meters, shown by the solid and dashed curves in Fig. 5, respectively.

In the present case, the curves A refer to a fully vegetated path, such as the one considered in Sec. 2 above. The curves B, however, refer to a path that lies partly through vegetation and partly through air. This may happen when the helicopter is concealed in a clearing or when it skirts the forest edge, but the radar antenna is well above the tree tops. Alternatively, the helicopter is above the trees, but the antenna is below the average tree height. In both cases, it has been assumed that the portion of the path through the vegetation is about equal to that through air, thus obtaining the

curves B. Finally, we show the free-space loss in curves C, i.e., no vegetation is present and the target is visible under line-of-sight conditions and ground lobing is disregarded.

To compute the curves in Fig. 5, we have used Eq. (7) of reference 4 for the radar equation, which yields

$$L = -10 \log \frac{\sigma}{4\pi} (\lambda G D)^2 , \qquad (4)$$

where: σ = radar cross-section of target;

G = antenna gain;

D = reduction in power due to propagation along a distance R between antenna and target.

To account for a realistic situation, we have assumed that the antenna aperture is fixed, so that the gain varies[4] as f^2, thus strongly favoring the higher frequencies. The reduction in power D was found by calculating $D \propto \exp(\alpha R)$, where α is measured in nepers via Eq. (2) and by properly accounting for a lateral wave when appropriate[4]. The curves in Fig. 5 were then calculated for a cross-section σ = 100 sq.meters, which value is representative of a small to medium size helicopter, and for a gain given by $G = 500 f^2$ with f measured in GHz. (i.e., G = 5 at 100 MHz. and $G = 5.10^4$ at 10 GHz.)

The effect of reducing the amount of foliage traversed by the propagation path is dramatically demonstrated by comparing curves A and B. In particular, we note that differences of 50 dB. or more can be obtained at frequencies of 1 GHz. or higher. Thus, by raising the antenna above the tree tops, the radar range R can be considerably increased. However, we also observe that even under the partly vegetated path given by the curves B, the radar loss L is considerably smaller as the frequency is decreased to 1 GHz. or lower.

In fact, we note that even though the free-space curves C show a preference for the higher frequencies, all of the curves A and B increase rapidly with frequency, especially for $f \geq 1$ GHz. This, we recall, occurs despite the fact that the antenna gain G was taken

proportional to the frequency squared. Of course, as the helicopter rises above the trees, the radar conditions vary gradually so as to go from curves B to curves C. However, until a clear line-of-sight is established between the radar antenna and the helicopter, the radar loss L appears to take extremely high values for frequencies greater than 1 GHz.

4. Capability of a Typical Radar System.

To cast the foregoing discussion into a proper perspective, it is worthwhile to estimate the restrictions imposed by vegetation on a typical radar system. For this purpose, we assume a radar which has the following specifications:

Transmitted power:	P_{tr}	= 1 kW.
Receiver bandwidth:	B	= 10 MHz.
Receiver noise figure:	N_f	= 10.
Antenna gain:	G	= $45/\lambda^2$.
Target cross-section:	σ	= 100 sq.meters.

Here σ and G are identical to those already assumed in Fig. 5, except that now G is expressed in terms of the wavelength λ (in meters) rather than in terms of f (in GHz.).

By using formula (4.22) of reference 5, the signal/noise ratio is given by

$$\frac{S}{N} = \frac{P_{tr}\, G^2\, \lambda^2\, \sigma}{R^4\, B\, N_f\, L_{t2}} \times 12.6 \times 10^{16} , \qquad (5)$$

where now all dimensions are measured in meters and frequencies in Hz. For a helicopter that hovers in a clearing or skirts the forest edge, the wave propagation path along R traverses entirely through vegetation if the antenna is at about tree-top level or below. The two-way terrain loss L_{t2} is then given simply by

$$L_{t2} = 40 \log e^{\alpha R} , \qquad (6)$$

where α must be measured in nepers.

A signal/noise ratio of unity determines the sensitivity limit of the system. This limit, in turn, yields a maximum range of detection R_{max}. By therefore taking S/N = 1 and solving for R, we obtain

$$R_{max} \exp(\alpha R_{max}) = 10^4 \left(12.6 \times \frac{P_{tr}\, G^2\, \lambda^2\, \sigma}{B\, N_f}\right)^{1/4} ,$$

which, for the values of P_{tr}, B, etc., assumed on the preceding page yields

$$R_{max} \exp(\alpha R_{max}) = 10^4 \left(12.6 \times \frac{10^3 \times 45^2 \times 100}{10^7 \times 10 \times \lambda^2}\right)^{1/4}$$

$$= \frac{2.245 \times 10^4}{\lambda^{1/2}} . \qquad (7)$$

The last result is a transcendental equation which may be solved for R_{max} by inserting, for any wavelength λ, the proper value of α (in nepers), which may be found from the idealized dot-dashed line in Fig. 2. The solution for our range of interest is then given in Fig. 6 by the solid line. It is noted therein that the maximum range R_{max} is 320 meters at 100 MHz. and this decreases to 65 meters at 10 GHz. Such a result demonstrates vividly that a radar system operating at the higher frequencies is considerably more affected by the presence of vegetation than a radar operating at the lower frequencies, despite the fact that the antenna gain (for an assumed constant-aperture antenna) was taken to be proportional to the frequency squared.

The above preference for the lower frequencies is further enhanced by the fact that, for $f \leq 1$ GHz., the actual propagation path is given by a lateral wave rather than a direct line through the vegetation[1-4]. In such a case, the terrain loss L_{t2} is not accurately given by Eq.(6) but, instead, we must use formula (36) of reference 1, which yields (for z and z_o not too close to the ground) a terrain loss

$$L_{t2}\ (\text{dB.}) = 40 \log \left(\frac{\pi |n^2 - 1|\ R}{\lambda} \right) \quad , \tag{8}$$

where n is the equivalent complex refractive index of vegetation. Inserting Eq. (8) into Eq. (5) and again solving for R_{max}, we get

$$R_{max} = \left(0.13 \times 10^{16} \frac{P_t\ G^2\ \lambda^6\ \sigma}{B\ N_f\ |n^2-1|^4} \right)^{1/8} \tag{9}$$

Taking a reasonable value of $n^2-1 = 0.03\ (1-j)$ and inserting the values already assumed before for P_t, G, etc., we get

$$R_{max} = \left(0.13 \times 10^{16}\ \frac{10^3 \times 45^2 \times \lambda^2 \times 100}{10^7 \times 10 \times 324 \times 10^{-8}} \right)^{1/8}$$

$$= 411\ \lambda^{1/4} \ . \tag{10}$$

By recalling that the lateral wave regime holds best at the lower frequencies (in this case, about 100-300 MHz.), we find that Eq. (10) yields the dashed line, which connects with the solid line at about 1 GHz. Because of the various approximations involved in deriving Eqs. (7) and (10), the latter equation was used to find a point for the dashed line only at 100 MHz., and the rest of the line was taken so as to join the solid line smoothly at 1 GHz.

If we now examine the dashed line for 100 MHz. $< f <$ 1 GHz., together with the solid line in the range $1 < f < 10$ GHz., it is evident that the increase in frequency between the two extremes of 100 MHz. to 10 GHz. causes a reduction in the detection range R_{max} by a factor of nearly 10.

It is worthwhile comparing the foregoing results to the free-space loss that holds, say, for the same helicopter at large heights above the ground. In that case, L_{t2} in Eq. (5) is unity. Solving for R_{max} in such a case is equivalent to replacing the term

exp (R_{max}) in Eq. (7) by unity, which yields

$$R_{max} = \frac{2.245 \times 10^4}{\lambda^{1/2}} \quad \text{(in meters).} \tag{11}$$

The last result implies that R_{max} varies from 13 km. at 100 MHz. to 130 km. at 10 GHz. Compared to these figures, the available value of R_{max} in the presence of vegetation is smaller by a factor of more than 20 even at the lower frequency end (100 MHz).

5. Conclusions.

The results illustrated in Fig. 6 clearly show that the propagation losses due to vegetation may reduce the radar detection range by several orders of magnitude. This reduction becomes more severe as the operating frequency is increased. In fact, even though larger antenna gains are available at the higher frequencies, the net detection range becomes actually smaller at these frequencies if a substantial portion of the radar-signal path traverses through vegetation.

On the other hand, the detection capability increases as the antenna is raised above the tree tops and/or the helicopter itself rises well above the forest. Ultimately, when the helicopter reaches a very high altitude, the radar-wave propagation path approaches free-space conditions and higher operating frequencies are then preferable. However, if the overall performance must include the detection of helicopters that fly so low that vegetated terrain intervenes between these targets and the radar antenna, the preference for the operating frequency is clearly towards the lower end.

Whereas the above conclusions indicate that radar systems should be designed to operate at lower frequencies, it must be emphasized that only propagation losses were considered here. Other considerations may influence the choice of an optimum frequency of operation and additional factors may favor higher frequencies. As an example, a Doppler radar system produces a return signal whose

Doppler frequency is proportional to the operating frequency. Because of clutter considerations, it is then desirable to increase this Doppler frequency, so that higher operating frequencies may then be needed. This, as well as other factors that may affect the overall sensitivity of the system, must be considered in conjunction with the propagation losses examined here when deciding on an optimum operating frequency. However, because the propagation losses are so rapidly increasing with frequency, it is believed that they will play a deciding role in choosing lower rather than higher frequencies for radar systems operating in forest environments.

REFERENCES.

1. T. Tamir, "Effect of a Forest Environment on the Performance of Doppler Radar Systems", U.S. Army Land Warfare Laboratory, Tech. Memo. No. LWL-CR-05P70, December 1971.
2. T. Tamir, "On Radio-Wave Propagation in Forest Environments", IEEE Trans. on Antennas and Propagation, vol. AP-15, pp. 645-648; September 1967.
3. D. Dence and T. Tamir, "Radio Loss of Lateral Waves in Forest Environments", Radio Sci., vol. 4, pp. 307-318; April 1969.
4. T. Tamir, "Frequency Dependence of Radio Losses for Radar Systems in Forest Environments", U.S. Army Land Warfare Laboratory, Tech. Memo. No. LWL-CR-05P70; July 1972.
5. D.K. Barton, "Radar System Analysis", Prentice-Hall, N.J., 1965.

March 20, 1974.

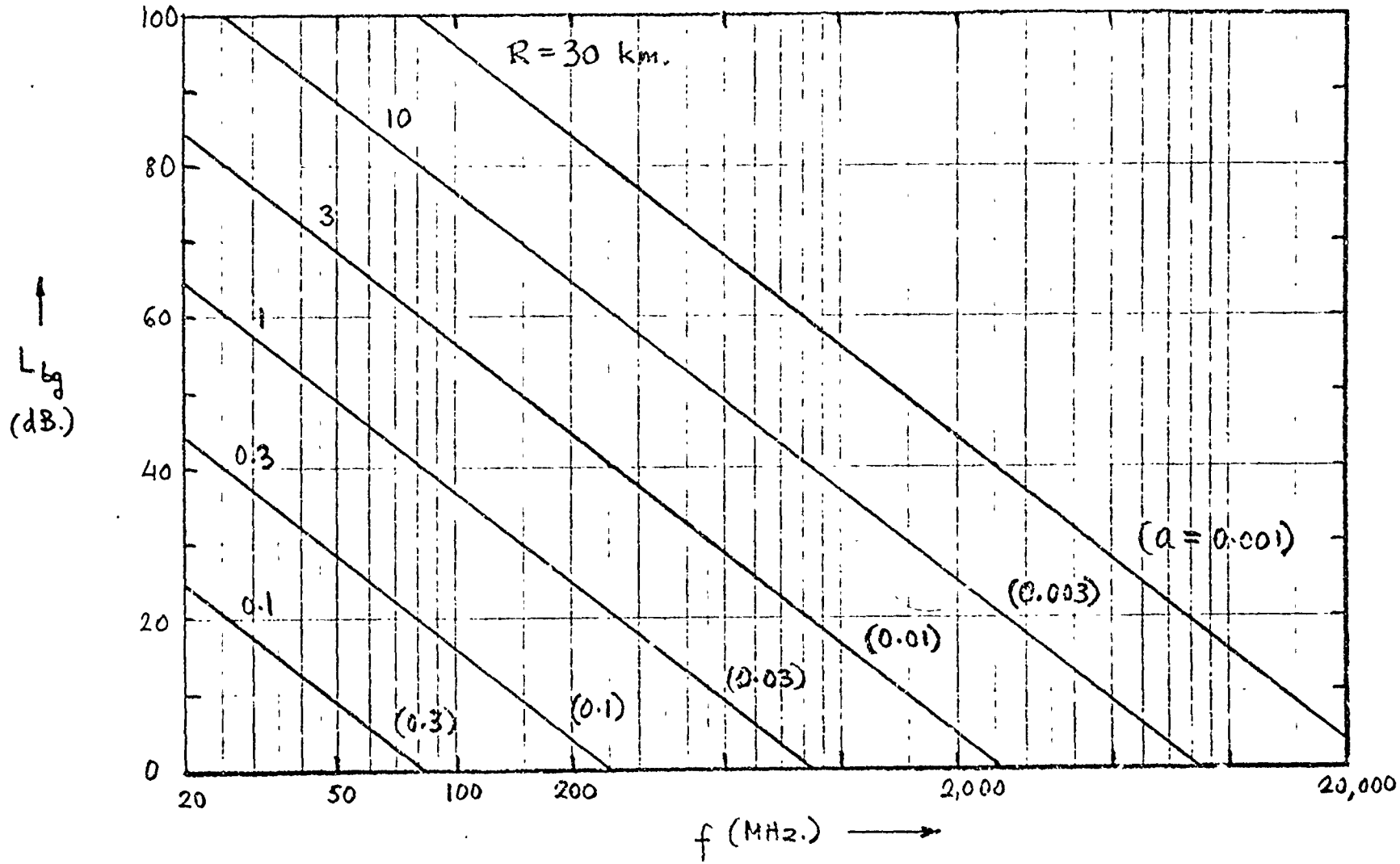

Fig. 1 - Two-way additional loss L_{bg} over bare-ground as a function of frequency, for $z = 3$ m., $z_o = 10$ m. and for various values of R. For other values of z, z_o and R, use the parameter $a = zz_o/R$ shown in brackets.

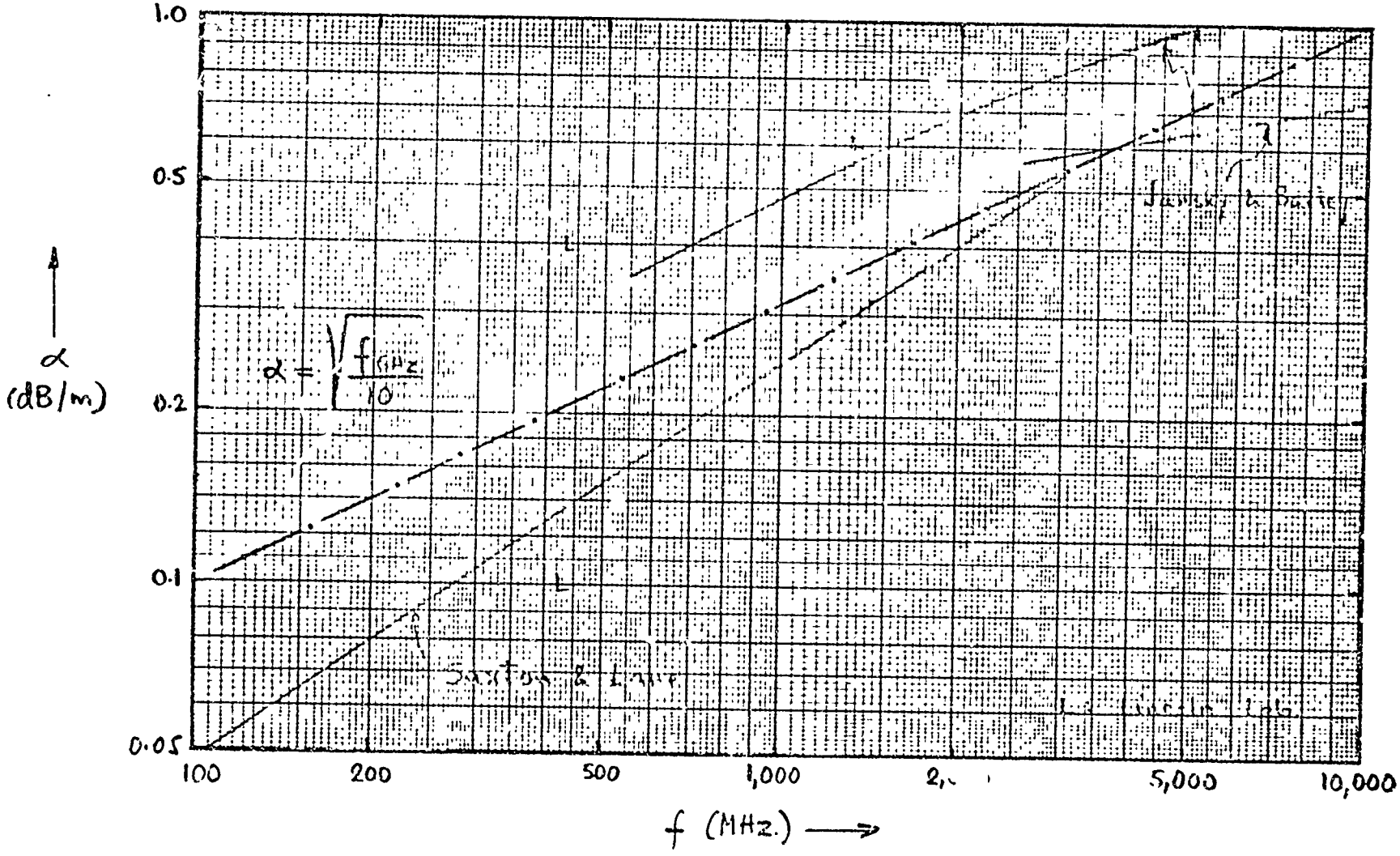

Fig. 2 - Frequency variation of the attenuation α through vegetation. The solid lines and points refer to measured data, as indicated; the dot-dashed line is a reasonable average, which is used as a simplified model.

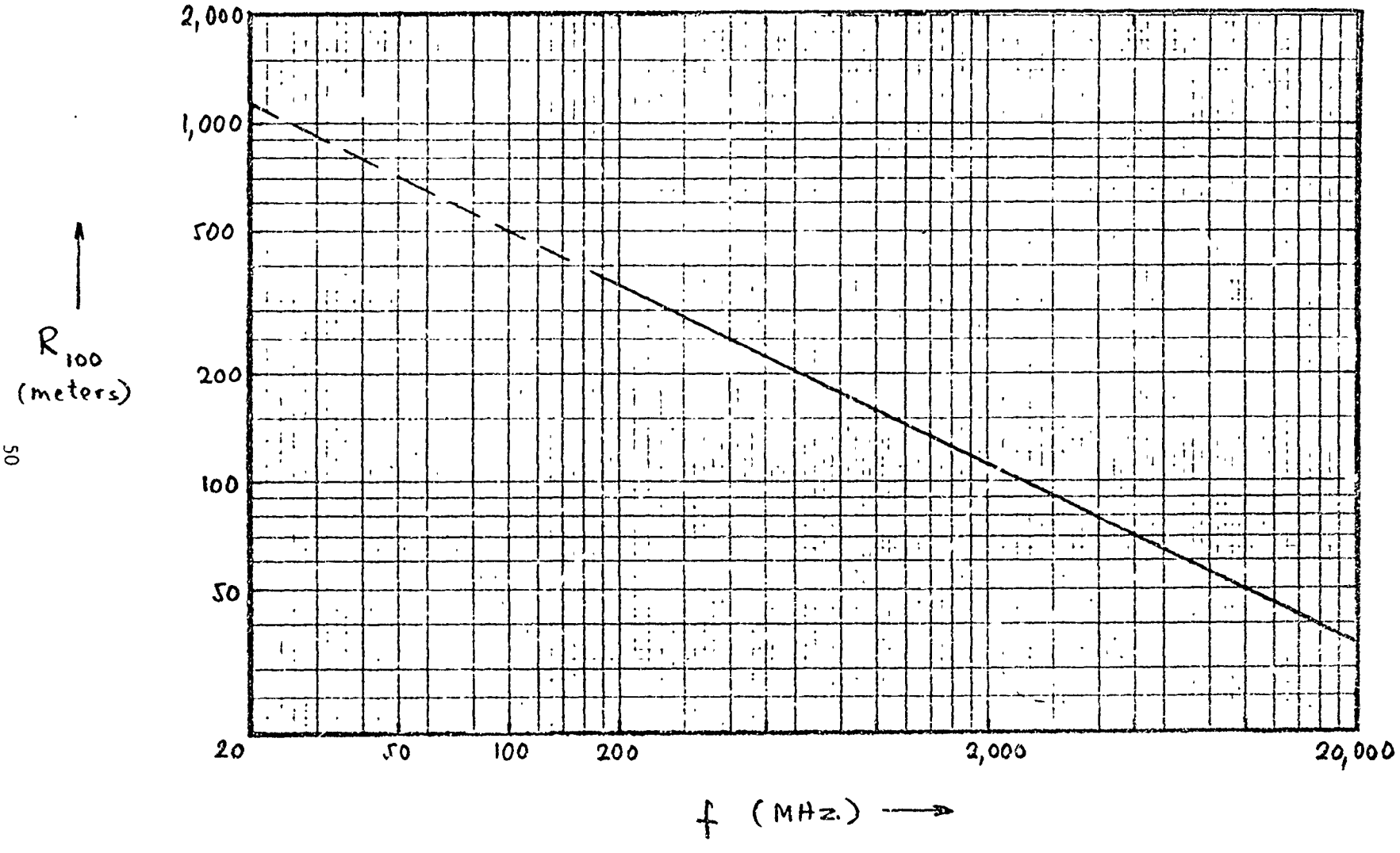

Fig. 3 - Distance R_{100} inside vegetation for a total two-way additional loss $L_{t2} = 100$ dB. The line shown is based on the model for α as given by the dot-dashed line in Fig. 2. The dashed portion of the line given here refers to the frequency range where propagation would usually occur via the lateral wave rather than through the vegetation, thus yielding a larger value of R_{100} than shown above.

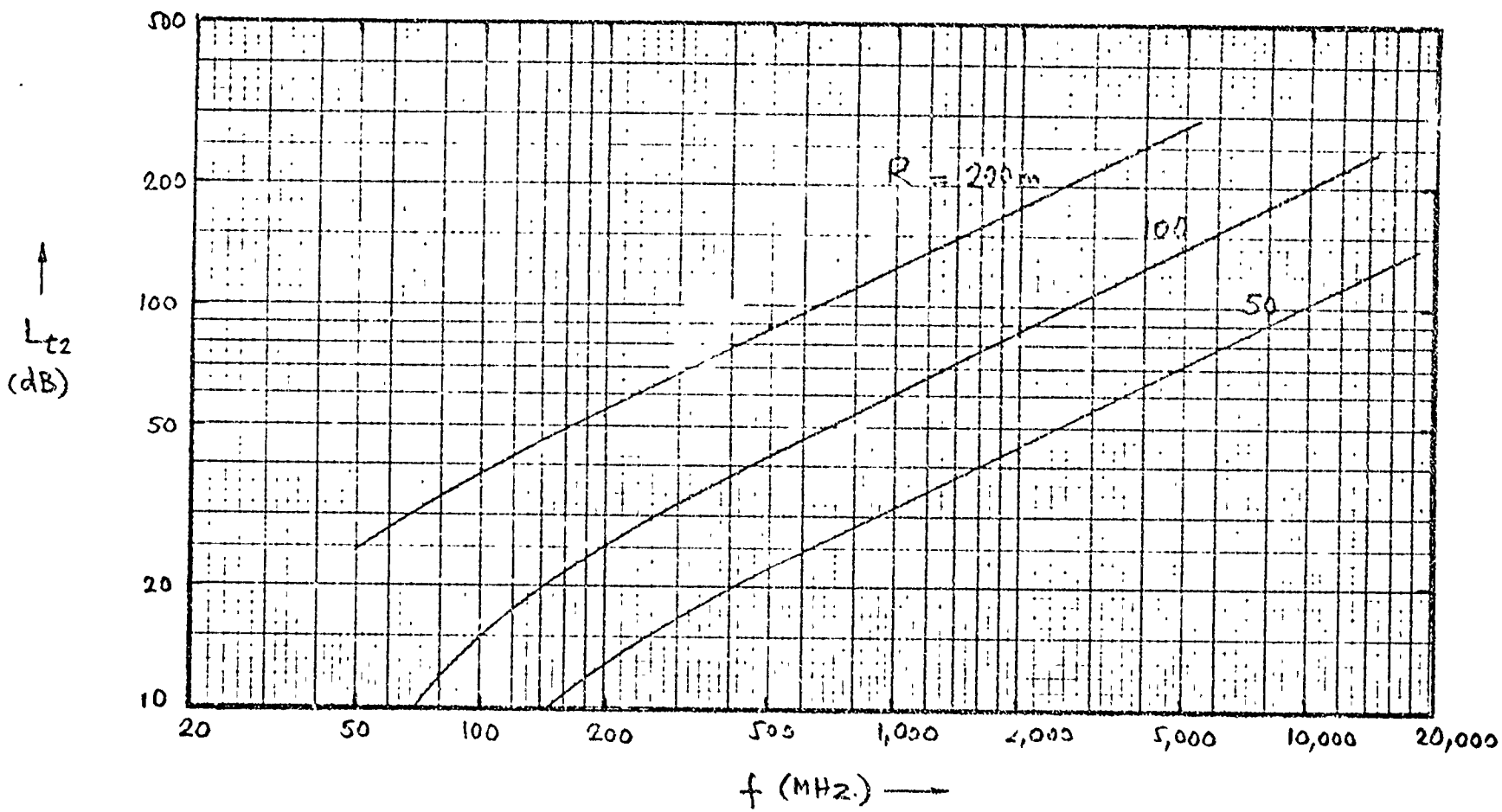

Fig. 4 - Estimated two-way additional loss L_{t2} due to vegetation for various distances R between antenna and target. The antenna is assumed to be close to the tree tops and the target is assumed to be below the tree tops.

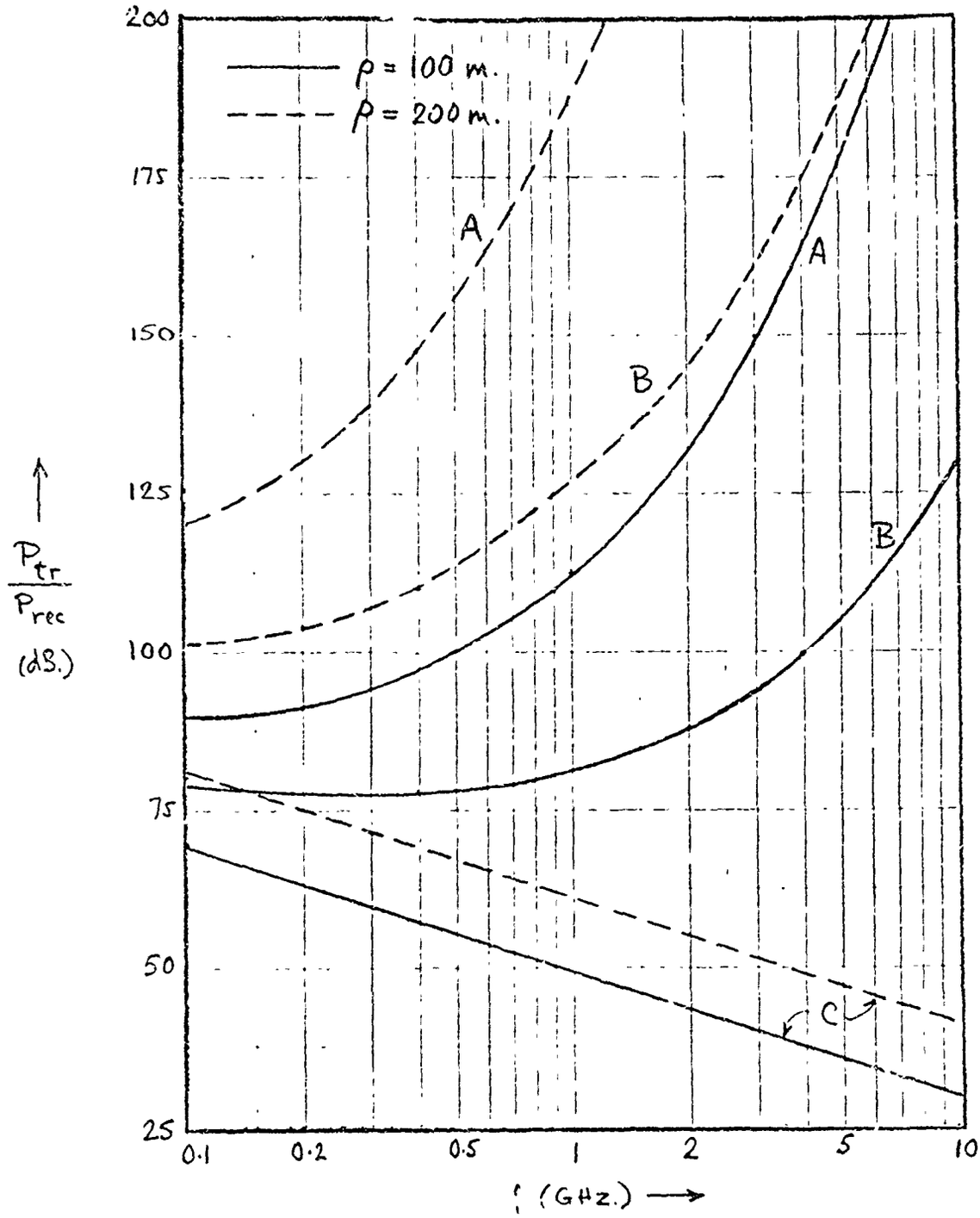

Fig. 5 - Estimated radar loss P_{tr} / P_{rec} as a function of frequency for the following cases:

A. Helicopter in a clearing, radar antenna near the tree tops;
B. As in A, but radar antenna 15 m. above the tree tops;
C. As in A or B, but no vegetation present (free-space conditions).

In all cases, the tree height h = 15 m., radar cross-section σ = 100 sq.m. and the antenna gain is assumed to vary as $G = 500\ f^2$ with f measured in GHz.

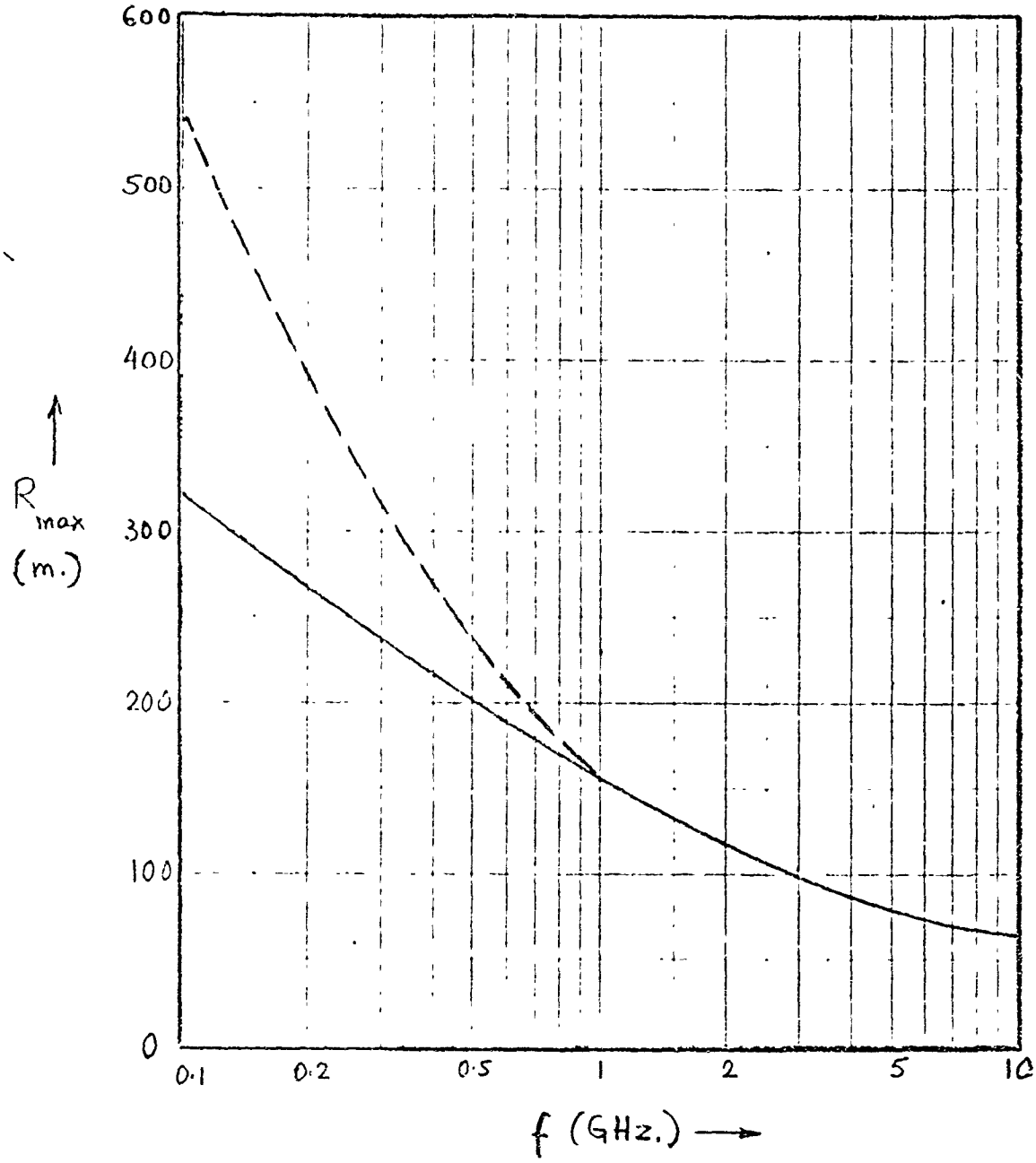

Fig. 6 - Maximum detection range R_{max} for a helicopter hovering in a clearing or skirting the forest edge. The radar antenna is assumed to be near the tree tops or lower and σ = 100 sq.m., P_{tr} = 1 kW., B = 10 MHz., N_f = 10 and G = 100 f^2, with f measured in GHz. The solid curve assumes a path through the vegetation, whereas the dashed line refers to lateral-wave conditions which prevail at the lower frequencies.